AWARD NUMBER: W81XWH-14-1-0219

TITLE: Novel molecular targets for kRAS downregulation: promoter G-quadruplexes

PRINCIPAL INVESTIGATOR: Tracy A. Brooks

CONTRACTING ORGANIZATION: University of Mississippi
University, MS 38677

REPORT DATE: November 2016

TYPE OF REPORT: Final

PREPARED FOR: U.S. Army Medical Research and Materiel Command
Fort Detrick, Maryland 21702-5012

REPORT DOCUMENTATION PAGE

Form Approved
OMB No. 0704-0188

1. REPORT DATE	2. REPORT TYPE	3. DATES COVERED
November 2016	Final	8/15/2014 – 8/14/2016

4. TITLE AND SUBTITLE
Novel molecular targets for kRAS downregulation: promoter G-quadruplexes

5a. CONTRACT NUMBER

5b. GRANT NUMBER
W81XWH-14-1-0219

5c. PROGRAM ELEMENT NUMBER

6. AUTHOR(S)
Tracy Brooks

E-Mail: tabrooks@olemiss.edu

5d. PROJECT NUMBER

5e. TASK NUMBER

5f. WORK UNIT NUMBER

7. PERFORMING ORGANIZATION NAME(S) AND ADDRESS(ES)

University of Mississippi
University, MS 38677

8. PERFORMING ORGANIZATION REPORT NUMBER

9. SPONSORING / MONITORING AGENCY NAME(S) AND ADDRESS(ES)

U.S. Army Medical Research and Materiel Command
Fort Detrick, Maryland 21702-5012

10. SPONSOR/MONITOR'S ACRONYM(S)

11. SPONSOR/MONITOR'S REPORT NUMBER(S)

12. DISTRIBUTION / AVAILABILITY STATEMENT

Approved for Public Release; Distribution Unlimited

13. SUPPLEMENTARY NOTES

14. ABSTRACT
The aim of this project was to characterize the biologically relevant non-canonical G-quadruplex (G4) structure within the promoter of the kRAS oncogene, and to determine the transcriptional regulation of the kRAS gene, particularly as it relates to the G4-forming region(s). Throughout the proposal, we elucidated a predominant G4 structure within the mid-G4-forming region of the promoter under varying co-solvent and nucleoplasm conditions, and described the structure as having mixed parallel/anti-parallel loops of lengths 2:8:10 in the 5'-3' direction. Using selective small molecules for the mid- and near-G4 regions, we further supported the ideal target for therapeutic development to be the mid-region structure. In support of aim 2, we examined the binding and functional effects of transcription factors predicted to bind to the G4-forming regions – Sp1, MAZ, and p53. While some of these silenced transcription, we expanded our search for activators to the entire promoter, examined the effects of E2F, AP1 and PPAR-gamma and searched for more interactive agents by LC-MS/MS.

15. SUBJECT TERMS
G-quadruplex, kRAS, Sp1, p53, MAZ, transcription factor

16. SECURITY CLASSIFICATION OF:			17. LIMITATION OF ABSTRACT	18. NUMBER OF PAGES	19a. NAME OF RESPONSIBLE PERSON
a. REPORT	b. ABSTRACT	c. THIS PAGE			USAMRMC
Unclassified	Unclassified	Unclassified	Unclassified	27	19b. TELEPHONE NUMBER *(include area code)*

Table of Contents

1. Introduction

The overall objective of this project is to characterize the formation and regulation of newly identified, biologically active, higher order DNA structures in the promoter of kRAS, which is a signaling molecule that has been shown to have aberrant activity in over 90% of pancreatic cancers. The higher order DNA structure under examination is a G-quadruplex, capable of forming in guanine-rich DNA regions found in regulatory regions of DNA, such as telomeres, centromeres, 5' UTR's and promoters. Generally these structures function to silence transcription, although each promoter structure requires individual examination for a functional determination. Within the kRAS promoter lies an extensive guanine-rich region of DNA with three separate putative G-quadruplex forming regions, which we have termed near, mid, and far in relation to their proximity to the transcriptional start site. The near region has been previously described, but we have shown it to be biologically inert, in contrast to the more distal mid-G4-forming region. The project focused on this newly identified DNA region, and has characterized the predominating isoforms under physiological conditions (Aim 1). Additionally, we have examined the transcriptional regulation of the kRAS promoter, with particular attention to the dynamic structures formed within the mid-G4-forming region, by the transcriptional regulators Sp1, MAZ, and p53 (both wild-type and mutant). Works extended to describe the effects on kRAS transcription by E2F, AP1, and PPAR-gamma, as well as a search for new promoter binding proteins. Cumulatively, findings from this proposal will have described a novel molecular target with detailed structural and regulatory information, enabling a concentrated drug discovery program with marked promise for new pancreatic cancer therapeutics.

2. Keywords:

G-quadruplex, kRAS, Sp1, p53, MAZ, transcriptional control

3. Accomplishments:

The **major goals** of this project were to *(1) Determine the predominant G4 structures within the mid- and far-regions of the kRAS core promoter*, and to *(2) Establish dynamic G4 regulation by candidate endogenous proteins.* Progress in these goals are as follows:

In the initial application, we presented biological data demonstrating basal expression changes and the effects of G4 induction with a luciferase plasmid containing the entirety of the kRAS promoter intact or with deletions of each G4-forming region. Conclusions from these plasmids led us to pursue the G4-formations in the mid- and

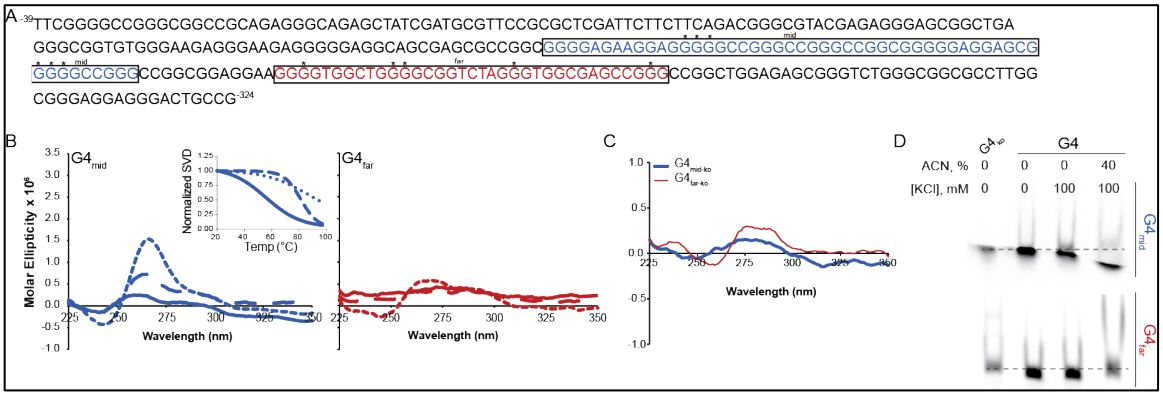

Figure 1. G4 formations in the extended *kRAS* promoter region. (A) The *kRAS* promoter shown from − 324 to − 39 bp relative to the transcriptional start site, contains distinct guanine-rich regions, termed near, mid, and far in the 5′–3′ direction; only mid- and far-were considered for this study; * denote G-to-T mutations within each region for knockout mutations shown in (C). (B) ECD was used to determine G4 formation and stability within each of these G4-forming regions in the absence (solid line) or presence of 100 mM KCl alone (long dash line) or in the presence of 40% acetonitrile (ACN) (short dash line). Thermal stability from 20 to 100 °C is shown in the inset of mid; the lack of strong G4 formation for $G4_{far}$ made melting not possible. (C) ECD demonstrated a lack of inducible G4 formation in the presence of 100 mM KCl with the selected G-to-T mutations in the knock-out (ko) sequences. (D) Electromobility shift assays were used to demonstrate the inter- versus intra-molecular G4 formations within each G4-forming region in the presence of 100 mM KCl with or without 40% ACN. A downward shifting of the DNA with the $G4_{mid}$ sequences, as compared to its linear ko sequences, indicates intramolecular structure formation, particularly evident in the presence of both cationic strength and dehydration. The $G4_{far}$ sequence, in the absence and presence of 100 mM KCl, demonstrates a downward shift from the linear ko sequence, but there is no difference between these two solvent conditions. In contrast, in the presence of KCl and ACN, there is a lack of a downward shift and the presence of retarded migration, as compared to control and KCl alone, indicating the potential for intramolecular G4 species.

far-G4-forming regions. However, the findings with the far-region were inconsistent with the G4-formation ex vivo. In this most distal region of the kRAS promoter, it was evident from electronic circular dichroism (ECD) and electrophoretic mobility shift assays (EMSA) that any G4 formation was between multiple strands of DNA – an intramolecular G4 (**Figure 1**).

Specific Aim 1: **Determine the predominant G4 structures within the mid- ~~and far-~~regions of the kRAS core promoter.**

Task 1.1: Determine the effect of varied physiological stressors, including chemical and mechanical, on G4 dynamics.

The most commonly studied stabilizing force for G4s is the presence of a monovalent cation, frequently KCl. We sought first to identify the effects of KCl-mediated G4 stabilization on the mid-forming region (**Figure 2**). Increasing KCl demonstrated a concentration-dependent effect on thermal stability (**Figure 2, bottom**), and an inverse relationship with G4 isoform distribution in that the more KCl present, the fewer isoforms noted (as demonstrated by a steeper slope). 10 mM KCl will be used in further studies with multiple forces to modulate G4 formation, and 100 mM will be used to mimic the most stable structure noted.

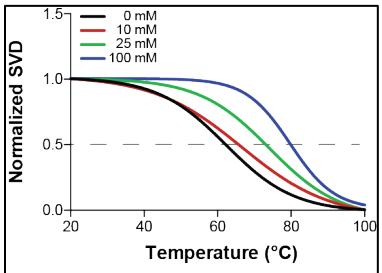

	0 mM	10 mM	25 mM	100 mM
T_M (°C)	62	67	74	80
Slope	-0.05	-0.04	-0.05	-0.07

Figure 2. Monovalent cationic effects on $G4_{mid}$ formation. $G4_{mid}$ was annealed in the presence of varying [KCl], mM. Thermal profiles (top) demonstrate a dose-dependent effect on G4 stability and isoform distribution (bottom). 10 mM KCl increases thermal stability of a broad base of structures, whereas 100 mM KCl markedly stabilizes fewer G4s.

The number of cycles used to prepare G4's from ssDNA can vary greatly, and can impact the structures formed. Therefore, we examined the effects of 1, 5, or 10 cycles of heating to 95 °C for 5 minutes, and cooling at 4 °C for 5 minutes. Spectra for all samples made it clear that the $G4_{mid}$ is a mixed parallel and antiparallel structure; more G4 formation occurred with more annealing cycles (**Figure 3, top**). Despite more G4 structures forming, it is clear by the thermal melting profile (**Figure 3, bottom**), both by the steepness of the melt (slope = -0.06, as compare to 0.03 and 0.02 for 5x and 10x annealing, respectively) and by the 50% formation temperature (67 °C, versus 47 °C and 66 °C for 5x and 10x annealing, respectively). As one cycle of annealing $G4_{mid}$ facilitates the most narrow and thermally stable structure, it was used for all future experiments.

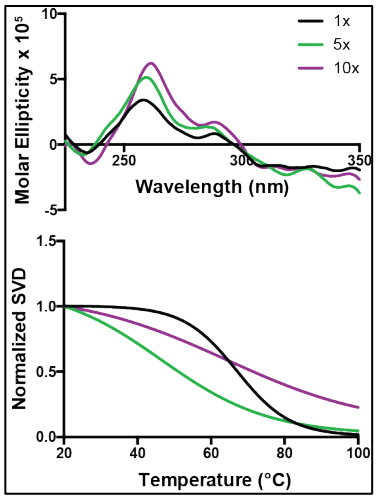

Figure 3. Number of melting cycles to isolate predominant $G4_{mid}$ species. $G4_{mid}$ was annealed and cooled 1, 5, or 10x in the presence of 100 mM KCl; spectra (top) and thermal melting profiles were obtained for each condition. All species were mixed parallel and antiparallel structures (top), and more structures were formed with an increase in heat and anneal cycles. From a thermal perspective, the two-state equilibrium, with a steeper thermal slope, is present only with a single heat/anneal cycle. This condition was used for all future experimentation.

Table 1	DT_M	Slope (D %)
PEG-300	38	-0.02 (-59)
ACN	3.3	-0.05 (+25)
Ficoll	-4	-0.06 (+34)
Glucose	0	-0.04 (-13)
Dextran	0	-0.04 (+/-0)
Glycerol	-1	-0.04 (-9)
Sucrose	0	-0.04 (-7)

Various dehydrating (acetonitrile, glucose, sucrose) and crowding (PEG-300, Ficoll, Dextran, Glycerol) co-solvents were incubated with the linear kRAS mid-G4-forming DNA (in the presence of 10 mM KCl) during the G4 annealing process from 0 – 40%. The saturating percentage for each co-solvent was determined, as described in **Figure 4**. At their saturating concentrations, the effects of each co-colvent on the thermal melt and isoform distribution was studied (**Table 1**). The sharpest slope, with minor changes in thermal stability, were noted with 10% ficoll (crowding) and 20% acetonitrile (dehydration). As ficoll was not noted, spectrally, to markedly increase G4 formation, and as the incorporation of acetonitrile in G4 studies is supported by other literature examples[1,2], studies were continued with acetonitrile.

DMS footprinting can reveal guanines involved in Hoogsteen base pairing. We performed this technique on the wild-type kRAS mid-G4 forming sequence in the absence and presence of 100 mM KCl (**Figure 5A-B**). Several partial patterns of protection were evident by DMS footprinting in the +KCl sample. To help elucidate a predominant structure from this equilibrium, we introduced G-to-T mutations in each of the seven runs of three or more continuous guanines. ECD was then run on each mutated sample including both spectra and thermal stability profiles in the presence of 10 mM KCl alone or with 20% acetonitrile, or with 100 mM KCl (**Figure 5C**). From the thermal profiles, it is clear that mutations in both runs B and F uniformly disrupt G4 formation. Double knockouts of runs B and F abrogate G4 formation (see $G4_{mid\text{-}ko}$ in **Figure 1C**). Also commonly leading to lower thermal stability were mutations in runs C and E. Cumulatively from these data a predominant G4 was modeled for $G4_{mid}$, having mixed parallel and anti-parallel loop directionality of lengths 4:10:8 in the 5'–3' direction, three tetrads stacked, and involving guanines in runs B, C, E, and F (**Figure 5D**).

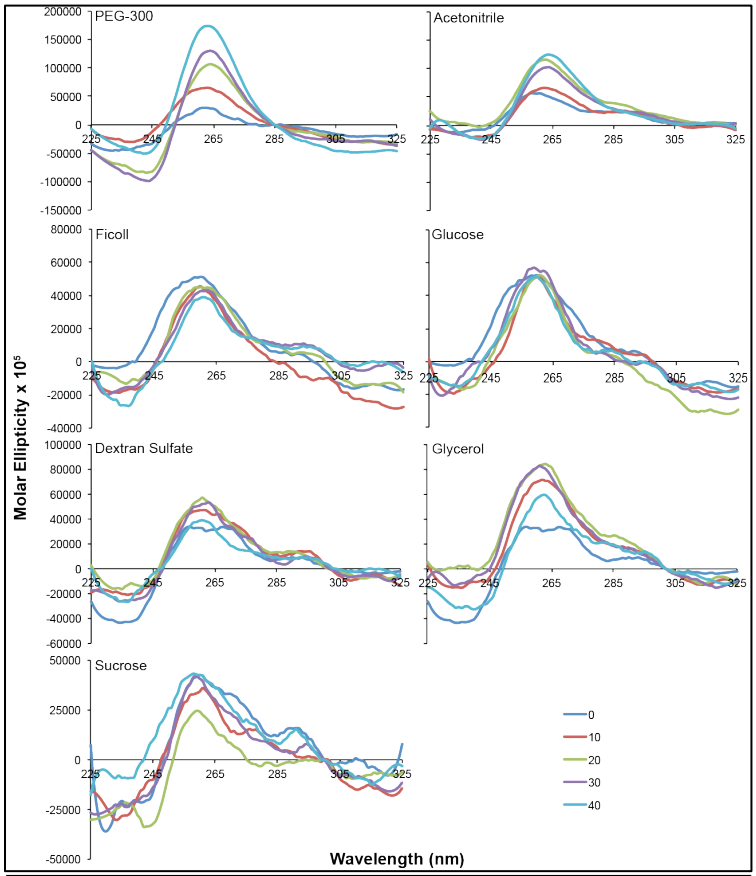

Figure 4. Dehydrating and Crowding co-solvent effects on $G4_{mid}$ formation. 0 – 40% of varying co-solvents were incubated with the DNA during the G4-annealing process. Spectral effects were measured and the percentile of each co-solvent saturating its effect was determined to be 10% for Glucose, 20% for Ficoll, Glycerol, Sucrose, Dextran Sulfate and ACN, and dual effects with PEG-300 at 20% and 40%.

Task 1.2: Determine the biological outcome of particular G4 formation within the kRAS promoter.

We engineered a series of luciferase plasmids containing the promoter region from -324 to +50 bp, relative to the transcriptional start site (TSS), or -500 to +0, relative to the TSS. In addition, sub-cloned plasmid were engineered, wherein G4-forming regions were mutated, rather than deleted as in the original proposal (**Figure 6**). In these studies, we used

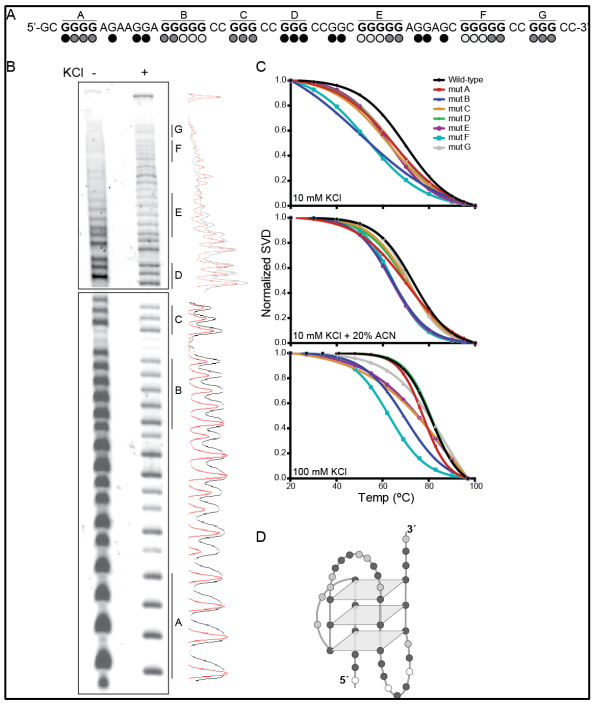

Figure 5. Predominant G4 isoforms formed within the mid-region of the kRAS promoter. (A) The $G4_{mid}$ sequence has seven runs of continuous guanines, A–G. The circles indicate evidence of protection in the subsequent DMS footprinting: light gray circles indicate marked protection, medium gray indicate partial protection, and black circles indicate DMS-mediated piperidine cleavage. (B) DMS footprinting of the mid promoter region of kRAS in the presence (+) or absence (-) of 100 mM KCl was performed. Images obtained from the top and bottom portions of the sequencing gel (boxed individually) were aligned, Image J software was used to graph and align histograms of the guanine cleavage pattern (no KCl = black line; 100 mM KCl = red line). (C) Thermal stability of a series of G-to-T mutants interrupting runs A–G, individually, of the $G4_{mid}$ sequence in the presence of 10 mM KCl alone (top), in the presence of 20% ACN (middle), or with 100 mM KCl (bottom). (D) Cumulatively, these data predict a G4 isoform formation of a tri-stacked structure incorporating runs B, C, E and F with intervening loops of 2, 10, and 8 bases in the 5'–3' direction. G = black circles, C = dark gray circles, T = light gray circles, A = white circles.

site-directed mutagenesis to introduce G-to-T mutations in both the near- and mid-G4 forming regions, but not the far based on the findings above (**Figure 1**). These mutations were designed to have minimal disruption on transcription factor binding sites but complete abrogation of G4 formation[3]. All kRAS promoter plasmids had basal expression values significantly different from the promoterless empty vector (EV) and the constituitively active SV40 plasmid, but were not significantly different from each other (**Figure 6B**). As was shown in the mid 1980's by Perucho, Jordano, and Yamamoto [4-6], transcriptional activation required the 0-+50 bp region, and was fine-tuned by the 0-500 bp region. Therefore this minor changes did not impact basal expression. When the pan-G4-stabilizing agent TMPyP4 was added to the kRAS-500 or kRAS-324 plasmids, significant decreases in promoter activity were noted. These changes did not occur with the control cationic porphyrin isomer TMPyP2, supporting a role for G4-stabilization (**Figure 6C**). A dose-response of TMPyP4 was performed with the EV, SV40, kRAS-324 and 324 mt Near and 324 mt Mid plasmids. The colorimetric contribution of this compound modulates luciferein-glow, as noted with the 50 mM effects in the EV and SV40 plasmids; when the dose-response of the compound was considered in each plasmid, the kRAS-324 and 324 mt Near, but not 324 mt Mid, plasmids demonstrated a dose-dependent decrease in promoter activity. The lack of TMPyP4-mediated silencing of promoter activity when the mid-G4-forming region was removed supported the basic premise of this study, which is that the optimal molecular target for G4-mediated modulation of kRAS expression is the $G4_{mid}$ structure.

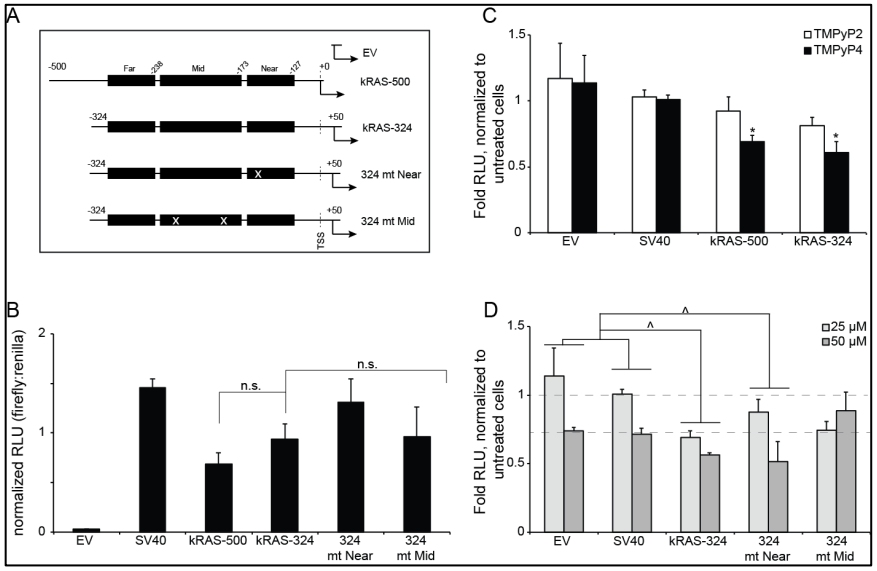

Figure 2. Isolating silencing G4 formations within the *kRAS* promoter. (A) A series of luciferase plasmids were constructed from the promoterless empty vector (EV) pGL4.17 backbone to localize the silencing G4s within the kRAS promoter. These included kRAS-500 (-500 – +0, relative to the transcriptional start site (TSS)), and kRAS-324 (-324 – +50 relative to the TSS). Site-directed mutagenesis of kRAS-324 was used to introduce G-to-T mutations (approximate location indicated with white x) that abrogate $G4_{near}$ (324 mut Near) or $G4_{mid}$ (324 mt Mid) formation. (B) Basal expression of the non-mutated plasmids was examined in transiently transfected HEK-293 cells for 48 hr and normalized to renilla expression in co-transfection assays. Promoterless (EV) and constitutively active (SV40) plasmids were included as comparison. There was no significant difference between the kRAS promoter plasmids. (C) The effects of HEK-293 treatment (48 hr) with 25 μM TMPyP2 and TMPyP4 on promoter activity was examined in the EV, SV40 and wild-type kRAS promoter containing plasmids kRAS-500 and kRAS-324. TMPyP4 was equally significant ($^{\#}p<0.05$ as compared to untreated control, per plasmid, as determined by one-way ANOVA) in lowering promoter activity in the two kRAS promoter plasmids, whereas it was inactive in the non-G4-containing EV and SV40 plasmids at that concentration. TMPyP2 was also inactive in all plasmids. (D) A TMPyP4 dose response (25 and 50 μM) was performed in the wild-type kRAS-324 plasmid and its two generated mutant plasmids 324 mt Near and 324 mt Mid. The dose response was performed in the non-G4-containing EV and SV40 plasmids. The colorimetric contribution of 50 μM TMPyP4 is evident in the EV and SV40 containing plasmids. In all plasmids where a dose-response was evident, the magnitude of that response was examined by a two-way ANOVA. Both kRAS-324 and 324 mt Near maintained significant ($^{\wedge}p<0.05$ for dose response, as compared to EV and SV40 effects) G4-mediated silencing of promoter activity, whereas 324 mt Mid did not. These findings indicate that G4-mediated silencing is contained within the mid-guanine-rich region of the kRAS promoter. All experiments were performed in a minimum of triplicate.

We next sought to use a surrogate marker to monitor the effect of G4 formation, rather than mutating the promoter sequence. We screened the Diversity Set II and III from the National Cancer Institute (NCI) by FRET Melt for compounds that selectively stabilized either the near- or the mid-G4 structure. From the screens, NSC 176327 emerged as a stabilizer for $G4_{near}$, and NSC 317605 was identified as a stabilizer of $G4_{mid}$. Both compounds harbored many similar traits to the previously identified and characterized G4-stabilizing compounds Quindoline i[7,8], NSC 338258[9], and several ellipticines[10]. Both compounds were tested for their G4 promiscuity, in comparison to TMPyP2, TMPyP4, Quindoline i, and the quindoline NSC

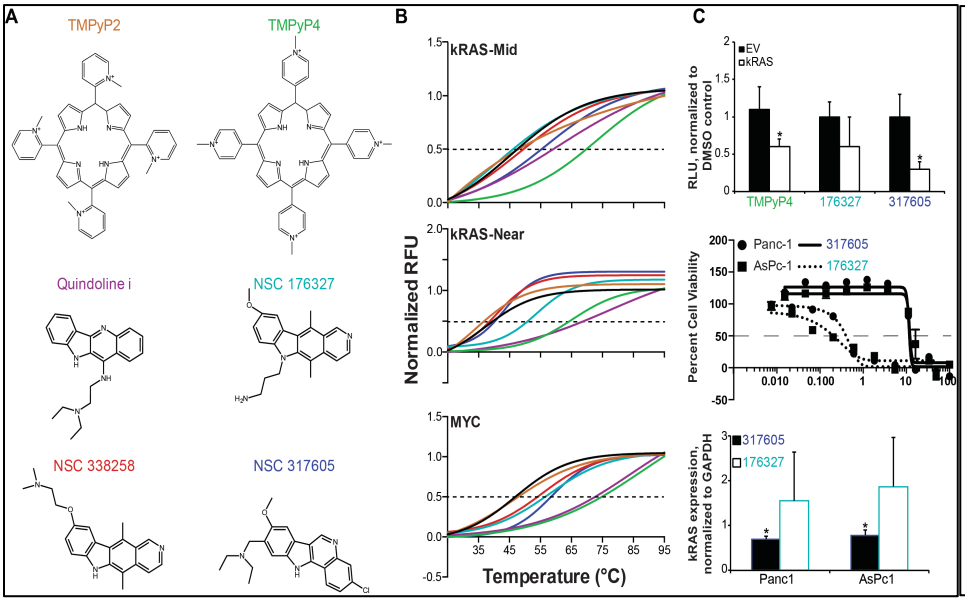

Figure 7. Selectivity and in vitro efficacy of compounds. (A) Structures of test G4 compounds used in (B) FRET Melt evaluation for thermal stabilization of the kRAS-mid, -near, and MYC G4s. Shifts to the right indicate thermal stabilization. (C) HEK-293 cells transfected with an EV or the kRAS-324 plasmid were exposed to 50 μM TMPyP4, 1 μM NSC 317605, or 1 μM 176327 for 48 hr (top). *p<0.05, vs control, by two-tailed t-test. The 24 hr IC_{50}'s of 317605 and 176327 in Panc-1 and AsPc-1 pancreatic cells were determined (middle). Cells were treated at their respective [IC_{50}] for 24 hr, and kRAS expression was monitored. Only 317605 significantly decreased kRAS expression in both cell lines (bottom). *p<0.05, vs control, by one-Way ANOVA.

338258 (**Figure 7A**) by FRET Melt using the kRAS-near, kRAS-mid, and MYC G4 sequences (**Figure 7B**). As expected, TMPyP2 was ineffective at stabilizing any of these G4s, whereas TMPyP4 significantly increased all of their thermal stability. Quindoline i, a previously identified MYC G4-stabilizing compound that was later shown to decrease MYC expression through a non-G4-mediated mechanism[7,8], stabilized all three G4s, but was least "active" against $G4_{mid}$. In agreement with previous literature[9], NSC 338258 stabilized only the MYC G4. NSC 176327 stabilized both the MYC and the $G4_{near}$, but **not** the kRAS-mid structure, whereas NSC 317605 stabilized $G4_{mid}$ and MYC, but not $G4_{near}$, structures.

The effect of stabilizing the mid-, but not near-, G4 on promoter regulation was examined in a luciferase system with no promoter (EV) or containing the full length kRAS promoter (kRAS [3]), as well as in pancreatic cancer cell lines harboring kRAS protein mutations – Panc-1 and AsPc1 (**Figure 7C**). TMPyP4 and NSC 317605 significantly decreased the promoter activity in the kRAS, but not the EV plasmid; NSC 176327 had no significant effects on either promoter. The effect or kRAS-mid stabilizing NSC 317605 and kRAS-near stabilizing NSC 176327 on cellular viability at 24 hr was measured by MTS in both cell lines, cells were treated with the IC_{50}'s and effects on kRAS mRNA expression was measured. Similar to the luciferase findings, NSC 317605 significantly lowered kRAS expression in both cell lines, whereas NSC 176327 did not. Changes in MYC expression was also monitored, as both compounds stabilized the MYC G4. At the IC_{50} doses in these cell lines, no change was noted with either compound (data not shown).

$G4_{mid}$ was incubated without or with 10 μM of NSC 176327 or NSC 317625 and subjected to DMS labeling and piperidine cleavage (**Figure 8**). Protection patterns clearly demonstrate a lack of protection of any guanines in the presence of NSC 176327, consistent with the lack of stabilization seen in **Figure 7B**, and the lack of biological effect seen in **Figure 7C**. In contrast, although a distinct pattern of G4-formation cannot be discerned, there is notable protection with NSC 317605 in runs B, C, and E. Future works will combine this compound with nucleoplasm (see below) in order to assign the predominant silencing G4 structure.

Figure 8. Varying stabilization of $G4_{mid}$ by small molecules. $G4_{mid}$ was incubated with 10 mM KCl alone or in the presence of NSC 176327 or NSC 317615 at 2.5 equivalences, each. Histograms of the DMS labeling and cleavage are shown on the right, with expanded sections of runs B-F.

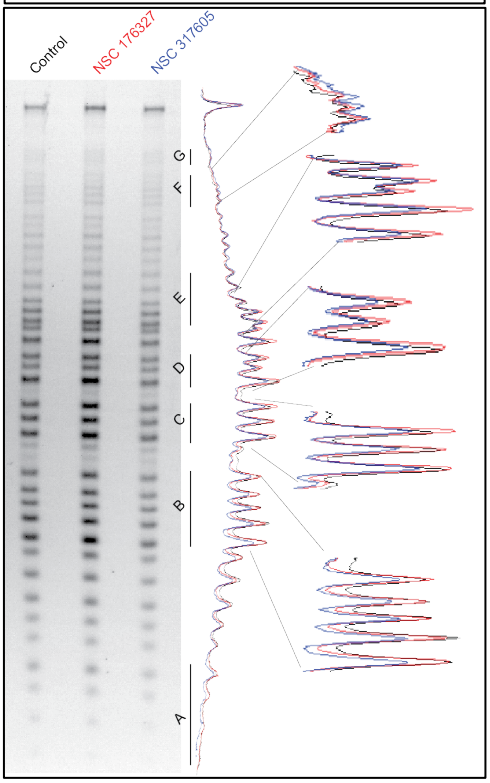

Task 1.3: Investigate the combined chemical stressors facilitating the predominant, and most biologically relevant, G4s within the mid- and far-regions of the kRAS promoter in a ssDNA system.

In addition to the co-solvent work described for task 1.1, we examined the effect of the most physiologically mimicking milieu able to be derived – extract nucleoplasm. A preparatory technique to isolate histones was modified to extrude those proteins and the DNA and to hold on to the remaining fraction. kRAS promoter mid-G4-forming DNA was then annealed into the G4 in the presence of increasing amounts of nucleoplasm (0 – 100%) and subjected to electrophoretic separation (**Figure 9A**). Using the dual B and F G-to-T mutation G4 knockout sequence as a control, it is evident that incubation with nucleoplasm at all concentrations facililitates intramolecular G4 formation. As the percentage increases, most notably at 40 and 100% nucleoplasm, the banding becomes more diffuse, which is indicative of a large number of competing isoforms. The isoform distribution was examined by ECD thermal melting profiles (**Figure 9B**) after the G4 was annealed one time in the presence of 10 mM KCl plus 2, 5, or 10% nucleoplasm. The thermal melts increased concentration-dependently from 57 to 71 to >100 °C. At the same time, though, the slope became less steep, moving from -0.14 to -0.05 to -0.02. So while more nucleoplasm mediated more thermal stability, there was a greater number of competing G4 isoforms present. From all of our studies with $G4_{mid}$ and co-solvents for physiological mimicry, 2% nucleoplasm is the best at decreasing the number of equilibrating G4 species.

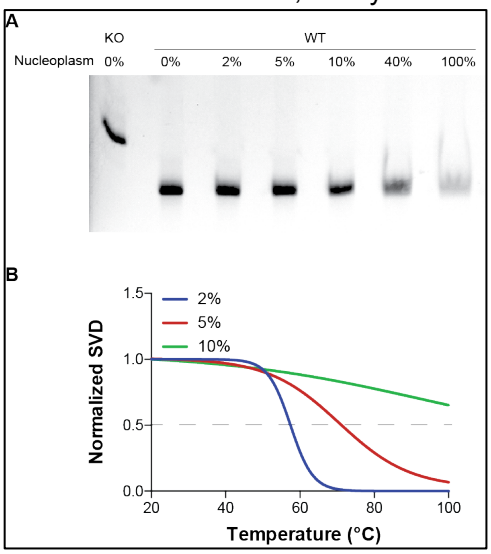

Figure 9. Effect of Nucleoplasm on $G4_{mid}$ formation. (A) Incubation with increasing amounts of nucleoplasm maintains an intramolecular G4 structure, although the pattern becomes diffuse with more equilibrating structures at 40 and 100%. (B) The effect of 2-10% nucleoplasm on G4 thermal profiles was examined. Thermal stability increases with more nucleoplasm, consistent with (A), but the number of isoforms is fewest at 2%.

Specific Aim 2: Establish dynamic G4 regulation by candidate endogenous proteins.

Task 2.1: Examination of protein binding to various DNA topologies and role of protein binding in structural equilibration.

At the onset of this project, we sought to follow up on literature reports on the effects of MAZ expression on kRAS transcription. It was published that MAZ positively regulated kRAS in Panc-1 cells, and determination that MAZ interacting with the near G4 structure. With our findings that $G4_{near}$ is not biologically active and that promoter silencing by a G4 structure is mediated by $G4_{mid}$, and the presence of MAZ binding sites in the mid-G4-forming region (**Figure 10**) , we sought to establish an interaction between $G4_{mid}$ and the MAZ protein. We induced $G4_{near}$ (for comparison with literature findings) and $G4_{mid}$ with 100 mM KCl and monitored MAZ (4 μg) binding by EMSA. Remarkably, we did not find any interactions between MAZ and either G4 structure (**Figure 11, left**). We tried several binding conditions, buffers, concentrations of protein, and this finding was consistent; we are unable to recapitulate the published data. Sp1 and MAZ overlap in binding consensus sequences, both have a number of predicted binding sites in the kRAS promoter (**Figure 10**), and Sp1 has been noted to bind higher order structures[11]. We also, therefore, sought to demonstrate the interaction between Sp1 and either the

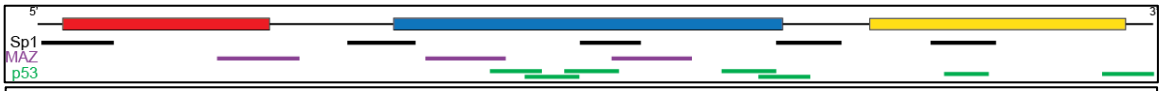

Figure 10. Putative binding sites of key proteins of interest (transcriptional activators Sp1, MAZ, and p53within the near, mid, and far regions of the *kRAS* promoter.

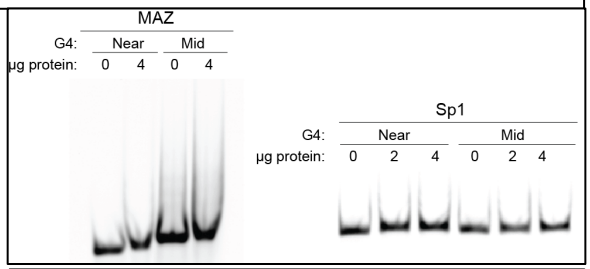

Figure 11. The binding of MAZ and Sp1 to FAM-labeled Near- or Mid-G-quadruplexes (as induced by 100 mM KCl) were examined. Neither protein, at concentrations up to 4 μg, demonstrated a supershift of the DNA, indicating there is no protein:DNA interaction.

near- or mid-region G4s (**Figure 11, right**). Similarly, no binding was noted with either G4. With these findings, we sought to understand the regulatory function of individual proteins (task 2.2) and to follow the function rather than the predicted interactions.

Task 2.2: Biological consequence of protein binding to kRAS promoter.

Consensus binding sites for a few proteins, which are also known to interact with higher order DNA structures[11-13], were identified (**Figure 10**). We monitored the effects of MAZ, Sp1, and p53 (wild-type and R273H mutant) in various intracellular contexts. We first overexpressed each of these proteins in HEK-293 cells that were also transfected with the kRAS-324 plasmid and a renilla control plasmid (pRL). MAZ, Sp1, and wild-type p53 all significantly decreased kRAS promoter activity, while mutant p53 had no effect (**Figure 12**). All samples were monitored by qPCR to ensure expression from the MAZ, Sp1, and p53 plasmids; mRNA expression increased in a dose-dependent manner in all cases.

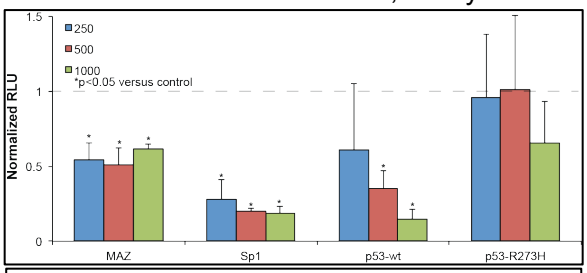

Figure 12. Protein regulation of kRAS promoter activity. Plasmids encoding for MAZ, Sp1, wild-type or mutant p53 (varying amounts) were co-transfected with kRAS-324 and pRL renilla plasmids. 48 hr later, luciferase was measured as a surrogate for kRAS promoter activity. MAZ, Sp1, and wild-type, but not mutant, p53 all significantly decreased (*p<0.05 as compared to no protein overexpression controls) promoter activity. n=3 independent experiments, each with internal n=2.

These proteins were further studied in PANC-1 pancreatic cancer cells, the same cells that were utilized in the literature. The effects with p53 – both wild-type and mutant – were highly variable and no significant changes in kRAS transcription were noted. Transfection with the MAZ protein mediating a three-fold increase in MAZ expression led to a ~25% in kRAS transcription; a 5.35-fold increase in Sp1 decreased kRAS transcription by more than 50% (**Figure 13**). These findings are consistent with the luciferase experiments above (**Figure 12**), but the findings with MAZ did not recapitulate literature reports[14]. The mechanisms mediating this decrease in transcription is unknown, as neither of these proteins bound either the mid- or the near-G4 forming region. Those mechanisms will be studied in the future.

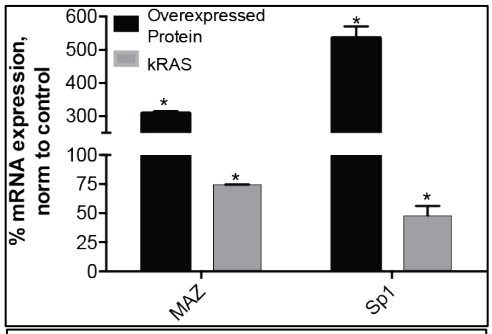

Figure 13. MAZ and Sp1 downregulate kRAS transcription in PANC-1 cells. Plasmids encoding for MAZ and Sp1 were transfected into PANC-1. Both proteins significantly decreased kRAS transcription, consistent with the luciferase findings. *p<0.05 as compared to control; n=3 individual experiments, each run in duplicate with qPCR duplicates of each sample.

Reports in the mid-1980's dissected the regions of the kRAS promoter required for kRAS transcription[4-6]. In addition to the -500 – 0 bp region, relative to the TSS, needed for full promoter activation, they identified the region from 0 – +50 as critical for kRAS expression. We thus expanded our search for kRAS regulatory proteins to include this region, both computationally, which identified E2F, and through reports of immunoprecipitation, which identified AP-2 and PPAR-γ. Plasmids expressing these proteins were co-transfected with the kRAS-324 and pRL plasmids into HEK-293 cells and luciferase function, as a surrogate for kRAS promoter activity, was evaluated 48 hr later. All three of these proteins significantly upregulated kRAS promoter activity, with the most remarkable activation noted by AP-2 (**Figure 14**).

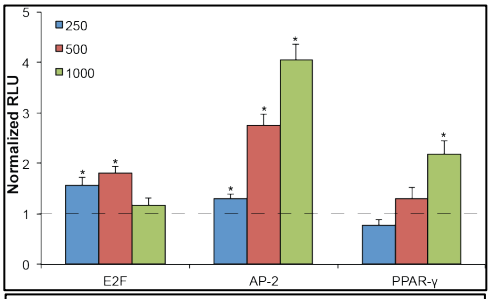

Figure 14. Increased kRAS promoter activity by transcription factors. Plasmids encoding for E2F, AP-2, or PPAR-γ (varying amounts) were co-transfected with kRAS-324 and pRL renilla plasmids. 48 hr later, luciferase was measured as a surrogate for kRAS promoter activity. Each protein significantly increased kRAS promoter activity at different transfection levels (*p<0.05 as compared to no protein overexpression controls) promoter activity. n=3 independent experiments, each with internal n=2.

The effect of AP-2, as well as MAZ and Sp-1, on endogenous kRAS expression was examined in an expanded pancreatic cancer cell line panel that included MiaPaCa-2 and AsPc-1 cells, which also express mutant kRAS. These three cell lines vary in their addiction to kRAS expression (Panc-1 < MiaPaCa-2 < AsPc-1), and in their basal expression of the proteins being studied (**Figure 15A**). The amounts of transfected plasmid for each cell line varied from 100-500 ng, each aimed at increasing mRNA of the respective gene by no more than 15-fold (**Figure 15B**). The effects of MAZ and Sp1 overexpression on kRAS transcription was consistent in all three cell lines, leading to a significant decrease ($p<0.05$ for all samples); AsPc-1, however, were the least responsive in agreement with that cell line expressing the highest basal amounts of both proteins (**Figure 15A**). The effect of AP-2 overexpression on kRAS promoter activation was not consistent for all three cell lines; a significant increase was only seen with MiaPaCa-2 cells and a significant decrease was noted with Panc-1 cells. Studies are continuing based on the findings from this grant to identify the transcriptional regulators of kRAS.

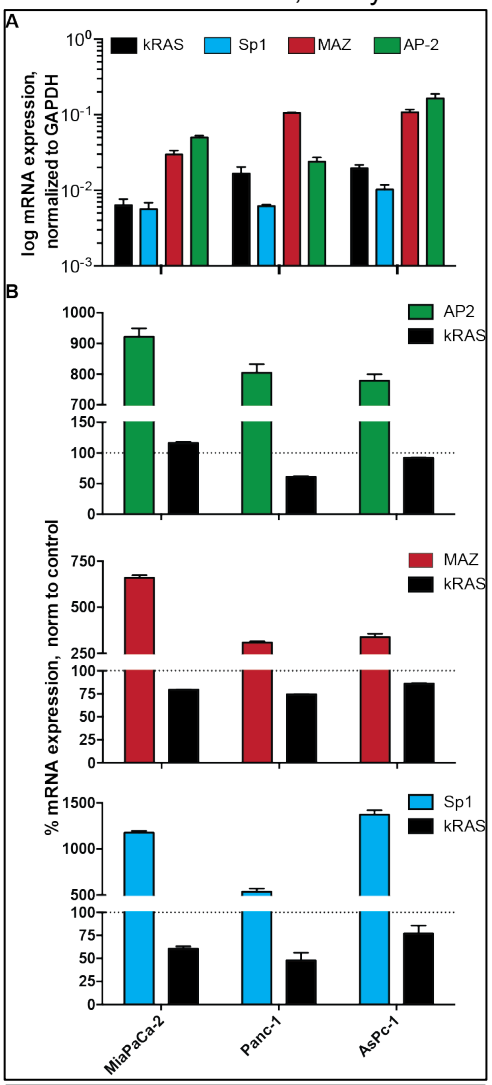

Figure 15. Increased kRAS promoter activity by transcription factors. (A) The cell lines vary in the basal expression of each of the proteins of interest, as shown by internal normalization to GAPDH. (B) Plasmids encoding for AP-2 (top), MAZ (middle) and Sp1 (bottom) were transfected into the pancreatic cancer cells such that their expression went up 3 – 15-fold. The effects of MAZ and Sp1 overexpression on kRAS transcription was consistent with the luciferase findings; AP-2 effects varied per cell line, leading to a significant increase in MiaPaCa-2 cells and a significant decrease in Panc-1 cells. No change was noted in AsPc-1 cells. n=3 for all experiments, with qPCR technical duplicates.

In a final study, we sought to identify proteins capable of interacting with the $G4_{mid}$ structure through a non-biased search. We formed the structure by annealing in the presence of 100 mM KCl, and incubated the G4 with nuclear lysate from Panc-1 cells. The proteins that bound the DNA were extracted from an agarose gel, with non-bound DNA and whole extract serving as controls. The resulting sample was subjected to LC/MS-MS identification of proteins, and a number of new leads were identified (**Table 2**). The experimental procedure is being repeated to ensure consistency, and the proteins with the greatest enrichment will be further studied.

Table 2.
hnRNP L
hnRNP A1
RNA helicase 1/2
NSEBP1
hnRNP M
PARP-1
Polypyrimidine tract BP

REFERENCES

1 Le, H. T. *et al.* Not all G-quadruplexes are created equally: an investigation of the structural polymorphism of the c-Myc G-quadruplex-forming sequence and its interaction with the porphyrin TMPyP4. *Organic & biomolecular chemistry* **10**, 9393-9404, doi:10.1039/c2ob26504d (2012).

2 Miller, M. C., Buscaglia, R., Chaires, J. B., Lane, A. N. & Trent, J. O. Hydration Is a Major Determinant of the G-Quadruplex Stability and Conformation of the Human Telomere 3' Sequence of d(AG(3)(TTAG(3))(3)). *J Am Chem Soc* (2010).

3 Morgan, R. K., Batra, H., Gaerig, V. C., Hockings, J. & Brooks, T. A. Identification and characterization of a new G-quadruplex forming region within the kRAS promoter as a transcriptional regulator. *Biochimica et biophysica acta* **1859**, 235-245, doi:10.1016/j.bbagrm.2015.11.004 (2015).

4 Jordano, J. & Perucho, M. Chromatin structure of the promoter region of the human c-K-ras gene. *Nucleic acids research* **14**, 7361-7378 (1986).

5 Jordano, J. & Perucho, M. Initial characterization of a potential transcriptional enhancer for the human c-K-ras gene. *Oncogene* **2**, 359-366 (1988).

6 Yamamoto, F. & Perucho, M. Characterization of the human c-K-ras gene promoter. *Oncogene research* **3**, 125-130 (1988).

7 Boddupally, P. V. *et al.* Anticancer activity and cellular repression of c-MYC by the G-quadruplex-stabilizing 11-piperazinylquindoline is not dependent on direct targeting of the G-quadruplex in the c-MYC promoter. *Journal of medicinal chemistry* **55**, 6076-6086, doi:10.1021/jm300282c (2012).

8 Ou, T. M. *et al.* Stabilization of G-quadruplex DNA and down-regulation of oncogene c-myc by quindoline derivatives. *Journal of medicinal chemistry* **50**, 1465–1474 (2007).

9 Brown, R. V., Danford, F. L., Gokhale, V., Hurley, L. H. & Brooks, T. A. Demonstration that drug-targeted down-regulation of MYC in non-Hodgkins lymphoma is directly mediated through the promoter G-quadruplex. *The Journal of biological chemistry* **286**, 41018-41027, doi:10.1074/jbc.M111.274720 (2011).

10 Lavrado, J. *et al.* KRAS oncogene repression in colon cancer cell lines by G-quadruplex binding indolo[3,2-c]quinolines. *Scientific reports* **5**, 9696, doi:10.1038/srep09696 (2015).

11 Raiber, E. A., Kranaster, R., Lam, E., Nikan, M. & Balasubramanian, S. A non-canonical DNA structure is a binding motif for the transcription factor SP1 in vitro. *Nucleic acids research* **40**, 1499-1508, doi:10.1093/nar/gkr882 (2012).

12 Adamik, M. *et al.* p53 binds human telomeric G-quadruplex in vitro. *Biochimie* **128-129**, 83-91, doi:10.1016/j.biochi.2016.07.004 (2016).

13 Petr, M. *et al.* Wild-type p53 binds to MYC promoter G-quadruplex. *Biosci Rep* **36**, doi:10.1042/BSR20160232 (2016).

14 Cogoi, S., Paramasivam, M., Membrino, A., Yokoyama, K. K. & Xodo, L. E. The KRAS promoter responds to Myc-associated zinc finger and poly(ADP-ribose) polymerase 1 proteins, which recognize a critical quadruplex-forming GA-element. *The Journal of biological chemistry* **285**, 22003-22016, doi:10.1074/jbc.M110.101923 (2010).

What opportunities for training and professional development has the project provided?

As a Career Development grant, training and development is a critical component of the aims. To this end, Dr. Brooks and her two graduate students working on this project were afforded opportunities to attend the annual national meetings of the American Association of Cancer Research in Philadelphia, PA (April, 2015) and in New Orleans, LA (April, 2016). At the 2016 meeting there was a large portion of time and resources dedicated to focusing on kRAS-related research, and the entire research team attended and extensively networked and expanded their development through these sessions. Dr. Brooks also attended the 2nd annual RAS Initiative symposium in Frederick, MD in December of 2015. This entire symposium was dedicated to RAS protein studies and enabled both the dissemination of our findings as well as new networking and collaborative connections. Students have also presented these works in a number of local and regional conferences, as listed below. In addition, Dr. Brooks served as a grant reviewer for the DoD BCRP funding mechanism, which is a remarkable mechanism for professional development in developing grant writing and reviewing skills.

How were the results disseminated to communities of interest?

For her outreach efforts, Dr. Brooks was invited to be the keynote speaker twice at the Pancreatic Cancer Action Network of Mississippi “Light the Night Purple” event in March of 2015 and 2016. She also serves as the Faculty Advisor to the University of Mississippi’s American Cancer Society’s Relay for Life Committee.

The manuscript and oral and poster presentations are described in “Products” below.

What do you plan to do during the next reporting period to accomplish the goals?

Nothing to report.

4. **Impact:**

Impact on the development of the G-quadruplex field.

The studies presented do contrast the findings of some literature reports. Namely, they highlight the importance of examining the entirety of a promoter region when examining transcriptional regulation by higher order DNA structures (e.g. looking at near, mid, and far-guanine rich regions, rather than only that in proximity to the transcriptional start site). While the near-G-quadruplex has been reported, through extensive promoter mapping of not only G-quadruplex formation, but also of *function* in the context of the entire kRAS core promoter, we were able to clarify that any silencing potential is held in the mid-region. This has a large impact on other groups that are pursuing drug discovery efforts focused on the near-region, which to date have been unsuccessful. The field will shift to pursue the mid-G-quadruplex in the near future. In addition, the field of kRAS studies has historically focused on mutant protein function, particularly as a target for therapeutic development. With these findings, a whole new target for therapeutic development has been described with applications to disease states reliant on the mutant protein (pancreatic, lung and colorectal cancers) as well as those with amplified kRAS (ovarian, testicular and triple negative breast cancers).

Impact on other disciplines.

Nothing to report.

Impact on technology transfer.

The plasmids made and utilized through this project have been requested by other universities so that they may optimize their compound screening efforts. MTA's are being drafted to share our resources, and we will deposit our major plasmids with AddGene for global availability.

Impact to society and technology.

Nothing to report.

5. **Changes/Problems:**

The only technical problem that arose during the funding period was combining chemical and torsional stress with luciferase plasmid footprinting. While a primer pair was optimized for promoter amplification (**Figure 16A-B**), incubation with those primers did not yield the anticipated PCR product size (**Figure 16C**). Studies of the plasmid will continue with any resources available to Dr. Brooks in order to meet this requirement, even outside of the scope of the funded period.

While not a change away from the original tasks, we did extend the scope of the protein regulation studies, since neither Sp1 nor MAZ were demonstrating activation of kRAS expression. To that end, we added E2F, AP-2, and PPAR-gamma into the proteins studied.

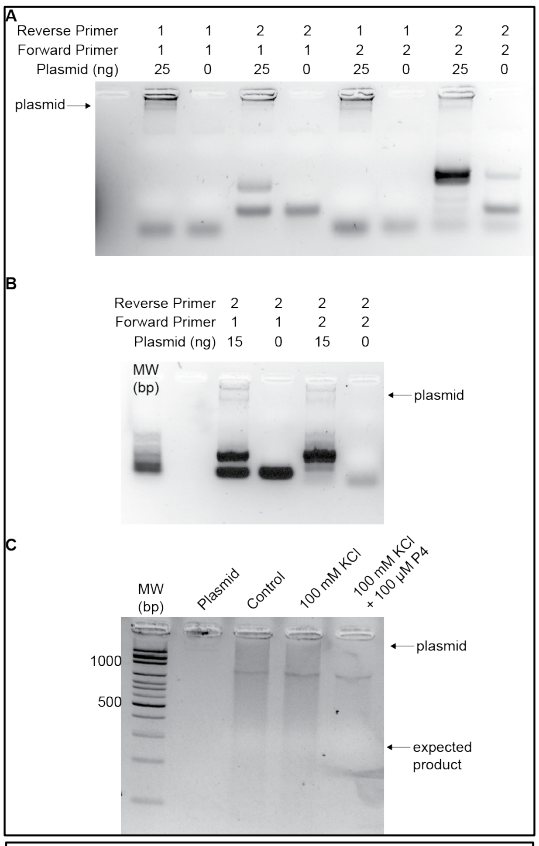

Figure 16. Primer optimization for plasmid DMS footprinting. (A) Two forward and two reverse primers were designed to amplify the G-rich region of the kRAS promoter and were tested in all four possible combinations with 25 ng of plasmid. (B) The two conditions with Reverse primer 2 were examined with 15 ng of plasmid to enhance product formation and decrease primer dimer. F2/R2 primers were deemed optimal. (C) kRAS-324 plasmid was incubated in buffer alone, with 100 mM KCl or with 100 mM KCl + 100 μM TMPyP4 before amplification with the F2/R2 primer pair. Larger than expected PCR products were identified (950 vs the anticipated 250 bp).

6. **Products:**

- **Publications, conference papers, and presentations**
  - **Journal Publications**
    - Morgan, RK; Batra, H; Gaerig, VC; Hockings, J; **Brooks, TA**. "Identification and characterization of a new G-quadruplex forming region within the kRAS promoter as a transcriptional regulator", *BBA-Gene*

Regulatory Mechanisms. 2016 Feb, 1859(2):235-245 PMID: 26597160

- **Books or other non-periodical, on-time publications**
  - Nothing to report
- **Other publications, conference papers, and presentations**
  - Batra, H; **Brooks, TA**. Binding and function of regulatory proteins to the kRAS promoter: a role in pancreatic cancer. 6th Annual Graduate Student Council Research Symposium. University, MS, April 2016. Oral presentation
  - Morgan RK; **Brooks, TA**. Targeting the kRAS G-quadruplex for transcriptional control as a potential therapeutic. 6th Annual Graduate Student Council Research Symposium. University, MS. April 2016. Oral presentation
  - Morgan, RK; **Brooks, TA**. Small Molecule Targeting of the kRAS Mid-G-Quadruplex for Potential Pancreatic Cancer Therapeutics. Proceedings of the American Association of Cancer Research (AACR), April 2016. Abstract 1254
  - **Brooks, TA**. The kRAS mid-promoter region G-quadruplex: Structure elucidation, protein regulation, and small molecule-mediated stabilization of a promising target for transcriptional downregulation. Second annual RAS Initiative Symposium, Frederick, MD, December 2015
  - Batra, H; **Brooks, TA**. The effect of transcription factors MAZ and Sp1 on kRAS transcription. University of Mississippi, School of Pharmacy, 19th Annual Poster Session, University, MS, October, 2015
  - Morgan, R; **Brooks, TA**. Targeting the kRAS G-quadruplex as a Novel Therapeutic Approach for Pancreatic Cancer. ACS Drug Discovery and Development Colloqium, University, MS, June 2015
  - Batra H; **Brooks, TA**. Unfolding the mystery of transcription factors associated with kRAS transcription. 42nd Annual MALTO Medicinal Chemistry – Pharmacognosy Meeting-in-Miniature, University, MS, May 2015
  - Morgan, RK; Rahman, KM; **Brooks, TA**. Selective Stabilization of the kRAS G-quadruplex: A Novel Therapeutic Target. 42nd Annual MALTO Medicinal Chemistry – Pharmacognosy Meeting-in-Miniature, University, MS, May 2015. Oral Presentation
  - Morgan, R; Rahman, KM; **Brooks, TA**. Structure Elucidation of G-Quadruplex within the mid-region of the kRAS Promoter and Identification of Stabilizing Small Molecules as Promising Transcriptional Silencers. Proceedings of the American Association of Cancer Research (AACR), April 2015. Abstract 1245.
  - Batra, H; **Brooks, TA**. The Effect of the transcription factor MAZ on kRAS transcription: a role for the G-quadruplex. Proceedings of the American Association of Cancer Research (AACR), April 2015. Abstract 2137.
  - Morgan, R*; Rahman, KM; **Brooks, TA**. Structure elucidation of G-quadruplex within the mid-region of the kRAS promoter and identification of stabilizing small molecules as promising transcriptional silencers. Mississippi Academy of Sciences Annual Meeting, Hattiesburg, MS. February 2015. *1st place poster winner*
  - Batra, H; **Brooks, TA**. The Effect of the Transcription Factor MAZ on kRAS Expression: A Role in Pancreatic Cancer. ACS Drug Discovery and Development Colloqium, Little Rock, AR. 2014.
  - Backus, K; **Brooks, TA**. A Novel Role for p53 in kRAS Binding in Pancreatic Cells. ACS Drug Discovery and Development Colloqium, Little Rock, AR. 2014.
- **Website or other Internet site**
  - Nothing to report

- **Technologies or techniques**
  - Nothing to report
- **Inventions, patent applications, and/or licenses**
  - Nothing to report
- **Other products**
  - Research materials have been made through this funded project that includes a series of luciferase plasmids driven by various regions and mutations of the kRAS promoter. These are available to the scientific community by request, pending MTA arrangements, and are to be deposited with AddGene for dissemination.

7. **Participants & Other Collaborating Organizations:**

Name:	*Tracy Brooks*
Project Role:	*Primary Investigator*
Researcher Identifier (e.g. ORCID ID):	0000-0002-1100-2437
Nearest person month worked:	*6*
Contribution to Project:	*Dr. Brooks has overseen all aspects of the research projects and guided the GRAs in their studies.*
Funding Support:	*No change*

Name:	*Rhianna Morgan*
Project Role:	*Graduate Research Assistant*
Researcher Identifier (e.g. ORCID ID):	
Nearest person month worked:	*12*
Contribution to Project:	*Ms. Morgan was responsible for all structural characterization work, including all aspects of Aim 1.*
Funding Support:	*No change*

Name:	*Harshul Batra*
Project Role:	*Graduate Research Assistant*
Researcher Identifier (e.g. ORCID ID):	

Nearest person month worked:	*12*
Contribution to Project:	*Mr. Batra was responsible for all protein regulatory studies, including all aspects of Aim 2.*
Funding Support:	*No change*

8. **Special Reporting Requirements:**

   There are no special requirements.

9. **Appendices**:

   There are no appendices to attach.

Biochimica et Biophysica Acta 1859 (2016) 235–245

Contents lists available at ScienceDirect

Biochimica et Biophysica Acta

journal homepage: www.elsevier.com/locate/bbagrm

Identification and characterization of a new G-quadruplex forming region within the kRAS promoter as a transcriptional regulator

Rhianna K. Morgan [a], Harshul Batra [a], Vanessa C. Gaerig [b], Jennifer Hockings [a], Tracy A. Brooks [a,*]

[a] School of Pharmacy, Department of BioMolecular Sciences, Division of Pharmacology, University of Mississippi, University, MS 38677, USA
[b] College of Pharmacy, Department of Pharmacology and Toxicology, The University of Arizona, Tucson, AZ 85721, USA

ARTICLE INFO

Article history:
Received 19 December 2014
Received in revised form 13 November 2015
Accepted 17 November 2015
Available online 18 November 2015

Keywords:
G-quadruplex
kRAS
Transcriptional control
Cancer therapeutics

ABSTRACT

kRAS is one of the most prevalent oncogenic aberrations. It is either upregulated or mutationally activated in a multitude of cancers, including pancreatic, lung, and colon cancers. While a significant effort has been made to develop drugs that target kRAS, their clinical activity has been disappointing due to a variety of mechanistic hurdles. The presented works describe a novel mechanism and molecular target to downregulate kRAS expression — a previously undescribed G-quadruplex (G4) secondary structure within the proximal promoter acting as a transcriptional silencer. There are three distinct guanine-rich regions within the core kRAS promoter, including a previously examined region ($G4_{near}$). Of these regions, the most distal region does not form an inducible and stable structure, whereas the two more proximal regions (termed near and mid) do form strong G4s. $G4_{near}$ is predominantly a tri-stacked structure with a discontinuous guanine run incorporated; $G4_{mid}$ consists of seven distinct runs of continuous guanines and forms numerous competing isoforms, including a stable three-tetrad stacked mixed parallel and antiparallel loop structures with longer loops of up to 10 nucleotides. Comprehensive analysis of the regulation of transcription by higher order structures has revealed that the guanine-rich region in the middle of the core promoter, termed $G4_{mid}$, is a stronger repressor of promoter activity than $G4_{near}$. Using the extensive guanine-rich region of the kRAS core promoter, and particularly the $G4_{mid}$ structure, as the primary target, future drug discovery programs will have potential to develop a potent, specifically targeted small molecule to be used in the treatment of pancreatic, ovarian, lung, and colon cancers.

1. Introduction

The *kRAS* gene, located on chromosome 12 at p12.1 [1], encodes for the $p21^{RAS}$ (kRAS) protein that participates in the Raf–MAP kinase pathway powering cell growth and apoptosis. Activated kRAS predominantly signals through the mitogen-activated protein kinase pathway (Raf/MEK/ERK), phosphoinositide 3′-kinases, RalGEF, phospholipase C, and MEKK1 [2]. The best characterized activation pathway for kRAS is via tyrosine kinase receptors like EGFR. Mutations in RAS proteins are found in approximately 30% of all human tumors, with *kRAS* being the most frequently mutated isoform [2,3]; such mutations render the protein constitutively active.

Single point mutations of the *kRAS* gene, frequently occurring in codons 12, 13, and 61, abolish GAP-induced GTP hydrolysis through steric hindrance (G12 and G13) or by interfering with coordination of a water molecule necessary for GTP hydrolysis (Q61) [4]. The highest incidence of mutational activation occurs in colorectal, ovarian, and lung cancers, and most notably in >95% of pancreatic adenocarcinomas [1,3]. kRAS mutations have been associated with increased tumorigenicity and poor prognosis [2]. Endogenous expression of mutant $kRAS^{G12D}$ was capable of inducing pancreatic intraepithelial neoplasias (PIN) in a mouse model [5]. In the absence of a mutation, increased kRAS activity in human tumors has been shown to be the result of gene amplification, overexpression, or increased upstream activation [2]. Targeting kRAS expression or activity is well validated to inhibit tumor cell proliferation.

While there have been many attempts to mitigate mutant kRAS activity, including farnesyltransferase inhibitors, Raf kinase inhibitors, and MEK inhibitors, no clinically relevant agent that specifically targets kRAS currently exists [1]. Studies have shown that a reduction in kRAS expression in cancerous cells, by antisense, miRNA or siRNA oligonucleotides, halts proliferation and leads to cellular death [6,7]. Furthermore, the inhibition of activated kRAS has been shown to revert malignant cells to a non-malignant phenotype, and cause tumor regression both in vitro and in vivo [2,8]. Transcriptional or translational downregulation of kRAS has been validated as a novel therapeutic approach [1,6,7], with great potential to succeed where previous efforts focused on modulating kRAS signaling did not [3]. However, achieving this downregulation therapeutically is currently hampered by the lack of a molecular target. The works presented highlight a viable new target to fill this gap.

* Corresponding author at: 307 Faser Hall, University, MS 38677, USA.
E-mail address: tabrooks@olemiss.edu (T.A. Brooks).

http://dx.doi.org/10.1016/j.bbagrm.2015.11.004
1874-9399/

The core promoter region of *kRAS* is encompassed within the region from +50 bp through −510 bp, in relation to the transcriptional start site (TSS). The DNA within this region is highly G/C-rich (~75%), putatively capable of forming higher order non-B-DNA structures, and contains two nuclease hypersensitivity elements [9–11]. Such G/C-rich regions preferentially cluster around the transcriptional start site throughout the genome [12], with a high prevalence in oncogenic promoters [13]. Negative superhelicity induced by transcription can promote local unwinding of these G/C-rich regions of DNA, which allows for the formation of secondary structures known as G-quadruplexes (G4s).

G4s form from guanine-rich sequences by binding together four guanines in a planar fashion by Hoogsteen hydrogen bonds. Three or more planar guanine tetrads are vertically stacked either with multiple strands interacting in an intermolecular formation ex vivo, or with one strand folding upon itself in the biologically relevant intramolecular isoform. Loops connecting the runs of three or more continuous guanines can be in either the parallel or antiparallel configuration, and are typically 1–9 base pairs in length, although they have been described up to 26 base pairs. G4s have received much attention recently in the cancer community as their prevalence within the genome is notably higher in oncogenic promoters. Formation of G4s in DNA has been shown to modulate transcription, and in RNA modulates translation. Formation of G4s in DNA has been recently shown to clearly form in vivo, where it modulates transcription [14–19]. Their more unique, non-B-DNA, structure and potential ability to regulate the transcription of a host of oncogenes make G-quadruplexes an attractive drug target.

The region of the *kRAS* promoter from −129 to −160 has been previously examined [20–23], and various G4 formations were shown to exist in equilibrium. Examination of the *kRAS* promoter revealed an extensive region of G-rich DNA covering almost 300 bases from the TSS, and including a total of three putative G4-forming regions separated by 17 and 12 nucleotides in the 5′–3′-direction, respectively. These include the aforementioned previously described near- (five G-tracts over 30 bp), and the newly described mid- (seven G-tracts over 53 bp), and far- (4 G-tracts over 35 bp) regions. Each of these regions' G4 formations and function within the *kRAS* promoter is explored through biophysical studies, and in vitro with endogenous regulation in Panc-1 pancreatic cancer cells, as well as with a series of luciferase plasmid constructs. Cumulatively from these studies, it is clear that a major silencing G4 is formed from the mid-G4 forming region of the *kRAS* promoter, and that it is this structure that represents a promising new molecular target. These works present a previously undescribed regulatory region of the core *kRAS* promoter, and initial step in the drug discovery process for new compounds aimed at targeting kRAS. The development of compounds that are more specific and potent stabilizers of the unique mid-G4 has great potential as anti-cancer therapeutics to advance the care of pancreatic, lung, and colon cancer patients.

2. Materials and methods

2.1. Materials

All oligonucleotides (Table 1) were purchased from Operon (Huntsville, AL). Acrylamide/bisacrylamide (29:1) solution and ammonium persulfate were purchased from Bio-Rad laboratories (Hercules, CA), and *N,N,N′,N′*-tetramethylethylenediamine was purchased through Fisher Scientific (Pittsburgh, PA). *Taq* DNA polymerase, T4 polynucleotide kinase, pRL-SV40 and pGL4.17 plasmids, and dual luciferase assay kits were purchased from Promega (Madison, WI). ^{32}P-ATP was purchased from NEN Dupont. All other chemicals, unless otherwise noted, were purchased from Sigma-Aldrich (St. Louis, MO).

2.2. Circular dichroism (CD)

CD spectra and thermal stability of all sequences (5 μM in 50 mM Tris–HCl, pH 7.4) in the absence and presence of KCl (up to 100 mM) and acetonitrile (ACN, up to 40% [24–29]), as indicated in the text, were recorded on an Olis DSM-20 Spectrophotometer fitted with a CD 250 Peltier cell holder (Bogart, GA) from 225 to 350 nm with scanning time as a function of high volts (<1 s/nm). Thermal stability was determined through collection of spectra (225–350 nm) from 20 to 100 °C (spectra recorded each 7 °C, sample held at temp for 1 min before spectral scan) and single value decomposition (SVD) analysis was performed [30], from which non-linear regression was used to determine the T_M. All spectra were baselined for signal contributions from the buffer.

2.3. Electrophoretic mobility shift assay (EMSA)

FAM-labeled oligonucleotides were denatured by heating to 95 °C for 10 min and then slowly cooled in 50 mM Tris–HCl, pH 7.4, with or without 100 mM KCl alone or with 40% ACN to induce G4 formation. After the addition of non-denaturing loading dye, samples were loaded on a 10% native polyacrylamide (29:1 acrylamide:bisacrylamide) gel, which was 50 V; the gel was visualized under blue light LED using a FotoDyne Investigator FX Imager.

2.4. Oligonucleotide end-labeling and purification

As indicated, DNA oligomers were 5′-end-labeled with [γ-^{32}P] ATP with T4 polynucleotide kinase for 1 h at 37 °C. The reaction was stopped by heating the samples to 90 °C for 5 min; the 5′-end-labeled DNA was purified with a Bio-Spin 6 micro-chromatography column (Bio-Rad Laboratories).

2.5. Dimethyl sulfate (DMS) footprinting

5′-end P- or 5′-FAM-labeled DNA oligonucleotides were denatured by heating to 95 °C for 5 min and then slowly cooled at 4 °C in 50 mM Tris–HCl buffer with or without monovalent cations. Following the

Table 1
Oligonucleotide sequences.

Name	5′–3′ sequence
PSA primer	TCGACTCTAAGCAAATGCGT
$G4_{near}$	AGGGCGGTGTGGGAAGAGGGAAGAGGGGGAGG
$G4_{near}$ DMS	TTTTTTTAGGGCGGTGTGGGAAGAGGGAAGAGGGGGAGGT TTTTTT
$G4_{near}$ FRET	[6-FAM]-AGGGCGGTGTGGGAAGAGGGAAGAGGGGGA GG-[TAMRA]
$G4_{mid}$	CGGGGAGAAGGAGGGGGCCGGGCCGGGCCGGCGGGGGA GGAGCGGGGGCCGGGC
$G4_{mid}$ DMS	[6-FAM]-TTTTTTTCGGGGAGAAGGAGGGGGCCGGGCCG GGCCGGCGGGGGAGGAGCGGGGGCCGGGCTTTTTTT
$G4_{mid}$ FRET	[6-FAM]-CGGGGAGAAGGAGGGGGCCGGGCCGGGCCGGC GGGGGAGGAGCGGGGGCCGGGC-[TAMRA]
$G4_{far}$	AAGGGGTGGCTGGGGCGGTCTAGGGTGGCGAGCCGGGCC
mut A	CGTTGAGAAGGAGGGGGCCGGGCCGGGCCGGCGGGGGA GGAGCGGGGGCCGGGC
mut B	CGGGGAGAAGGAGGTGGCCGGGCCGGGCCGGCGGGGGA GGAGCGGGGGCCGGGC
mut C	CGGGGAGAAGGAGGGGGCCGTGCCGGGCCGGCGGGGGA GGAGCGGGGGCCGGGC
mut D	CGGGGAGAAGGAGGGGGCCGGGCCGTGCCGGCGGGGGA GGAGCGGGGGCCGGGC
mut E	CGGGGAGAAGGAGGGGGCCGGGCCGGGCCGGCGGTGGA GGAGCGGGGGCCGGGC
mut F	CGGGGAGAAGGAGGGGGCCGGGCCGGGCCGGCGGGGGA GGAGCGGTGGCCGGGC
mut G	CGGGGAGAAGGAGGGGGCCGGGCCGGGCCGGCGGGGGA GGAGCGGGGGCCGTGC

addition of 1 μg of calf thymus DNA, the solutions were subjected to dimethyl sulfate (0.3% DMS in 1% ethanol) for up to 18 min. Each reaction was quenched in 0.3 M NaOAc and 0.2 M β-mercaptoethanol. The reactions were subjected to a preparative gel and each band of interest was excised and eluted. After ethanol precipitation and treatment with 1 M piperidine, the DNA was dried and washed with water, resuspended in a 95% formamide loading dye, and heated to 95 °C for 5 min before snap-cooling on ice. The cleaved products were separated on a 16% sequencing gel. Gels of $G4_{near}$ with ^{32}P-DNA were then dried and exposed to a phosphorscreen and imaging was performed with a Storm 820 phosphorimager. Footprinting gels for FAM-labeled $G4_{mid}$ were imaged under blue LED excitation and filtered through a blue emission filter on a FotoDyne Investigator FX Imager (Hartland, WI). Due to the size of the gels, they were imaged by the top and bottom regions, which were aligned using Adobe Illustrator; the images differentially obtained are distinguished by boxed outline in Fig. 3.

2.6. FRET melt assay

Thermodynamic stabilities of G4 DNA were performed using a fluorescence resonance energy transfer (FRET) melting assay [31]. Oligonucleotides were dual-labeled with 6-FAM on the 5′ end and a TAMRA quencher on the 3′ end (Operon for $G4_{near}$ and Midland Certified Reagent Company, Midland, TX for $G4_{mid}$). Stock concentrations of DNA were made in autoclaved, nuclease-free water at an approximate concentration of 100 μM. Assay concentrations and conditions were as reported; briefly, 200 nM of dual-labeled DNA was diluted in a 10 mM lithium cacodylate buffer (pH 7.2) supplemented with 10 mM potassium chloride, heated to 95 °C for 10 min, and allowed to anneal to room temperature slowly. Annealed DNA probe was then plated with 1 μM compound in a 96 well plate; fluorescence was recorded every 1 °C from 25 to 95 °C on a Bio-Rad CFX Connect qPCR machine (Bio-Rad, Hercules, CA). The melting temperature for 50% of the probe (T_M) was determined with GraphPad Prism 5.0 using non-linear regression modeling (GraphPad Software, Inc., La Jolla, CA).

2.7. Cellular viability assay

Pancreatic cancer Panc-1 cells were obtained fresh from ATCC (Manassas, VA), and were maintained in Dulbecco's minimal essential medium supplemented with 10% fetal bovine serum and 1× penicillin/streptomycin solution at 37 °C, in a humidified atmosphere containing 5% CO_2, in exponential growth. For cellular viability assays, cells were seeded in 96-well plates at a concentration of 7.5×10^3 cells per well in 90 μL of media, and allowed to attach overnight. The following day, a 10× stock plate of TMPyP2 or TMPyP4 diluted from 5 mM over a 5–6 log range in 0.5 log steps was made and 10 μL of this stock was added to the cell plate, in triplicate. The final high dose range was 0.08–500 μM. Cell-free wells with the same dose-range were plated, and served as measurements of background absorption. 48 h later, 20 μL of MTS + 5% PMS was added to each well and incubated for ~2 h before the absorption at 490 nm was measured on a BioTek Synergy 2 plate reader (Winooski, VT) [32]. In parallel, media was removed from all wells and replaced with 100 μL of fresh media before the addition of MTS as above. Background absorptions were subtracted, and data were normalized to control cells; IC_{50} values were determined with GraphPad Prism software (San Diego, CA) using non-linear regression modeling.

2.8. qPCR

Panc-1 cells were plated in 6-well plates at a concentration of 2×10^5 cells per well in 1 mL of media, and were allowed to attach overnight. The following day, the media was changed to contain either vehicle, or 25 μM TMPyP2 or TMPyP4. 48 h later, RNA was harvested from the cells using the Thermo Scientific GeneJet RNA Purification kit (Fisher Scientific); yield and quality were determined with a NanoDrop 2000, and only samples with 260/230 values >2 were used for further analysis. cDNA was synthesized with the Bio-Rad iScript cDNA synthesis kit, and qPCR was run on a Bio-Rad CFX Connect real-time PCR detection system using TaqMan primers from ABI (kRAS:hs00364282_m1, GAPDH:hs99999905_m1). kRAS mRNA expression was normalized to GAPDH, and to untreated control by the ΔΔCq method. Experiments were run in triplicate with internal technical duplicates; one-way ANOVA with post-hoc Tukey analysis was used to determine statistical significance.

2.9. Plasmid construction

A series of luciferase plasmids was constructed on the backbone of pGL4.17 plasmid (Promega). The promoter regions of interest, as denoted in Fig. 5, were inserted between the Bgl I (kRAS-500 plasmid) or Nhe I (all kRAS-324 plasmids) and HIND III cut sites. kRAS-324 was constructed by Operon; the kRAS-500, 324 mt Near, and 324 mt Mid constructs were created in-house according to previously published methods [33,34] or by site-directed mutagenesis with Q5 Site Directed Mutagenesis Kit (New England BioLabs, Ipswich, MA), respectively. The MYC-promoter containing Del4 luciferase plasmid was obtained from Addgene (Cambridge, MA).

2.10. Transfection and luciferase assays

HEK-293 cells were maintained in Dulbecco's minimal essential medium supplemented with 10% fetal bovine serum and 1× penicillin/streptomycin solution at 37 °C, in a humidified atmosphere containing 5% CO_2, in exponential growth. Before transfection with luciferase plasmids, cells were seeded in six-well plates at a concentration of 2×10^5 cells per well, and allowed to attach overnight. Each well was co-transfected with the plasmid of interest (500 ng) and the reference renilla plasmid pRL-SV40 (125 ng) with FuGene HD (Promega) in a 3:1 ratio with cells in OptiMEM medium (Invitrogen; Grand Island, NY). An unmodified pGL4.17 plasmid (Empty Vector, EV) and a constitutively active SV40-driven pGL4.13 plasmid were used as control vectors. Transfections were maintained at 37 °C in a 5% CO_2 humidified environment overnight before media was replaced with DMEM ± TMPyP2 or TMPyP4 in dark conditions, as the compound may be activated to a photosensitizer. After 48 h of incubation, the expression of firefly, with respect to renilla, luciferase was determined with the Dual Luciferase Assay kit (Promega); light output was measured with a Lumat LB9507 luminometer. All experiments were performed with biological triplicate with internal technical duplicates. Statistical significance was determined by a one-way ANOVA with post-hoc Tukey post-hoc analysis, or a two-way ANOVA, as indicated in the text.

3. Results

3.1. New G4-forming regions within the kRAS promoter

The core promoter region of kRAS is encompassed in the region from −510 to +50 bp surrounding the TSS [9–11], and contains cis-regulatory elements [34] and silencing G4 elements [33]. Examination of the entire 500 bp upstream promoter revealed two previously undescribed putative G4-forming regions in addition to the previously described region [20,21,33] (Fig. 1A). Herein, we term the known 32-bp sequence, found −128 bp from the TSS, as the near region, forming $G4_{near}$, the next distal region from −174 to −226 as the mid-region, forming $G4_{mid}$, and the furthest region from −238 to −273 as the far region, potentially forming $G4_{far}$. The mid-region consists of 52 bases and seven runs of three or more continuous guanines with intervening loops of 2–7 nucleotides, and the far region consists of 35 bases and four runs of three or more guanines with intervening loops of 5–9 nucleotides.

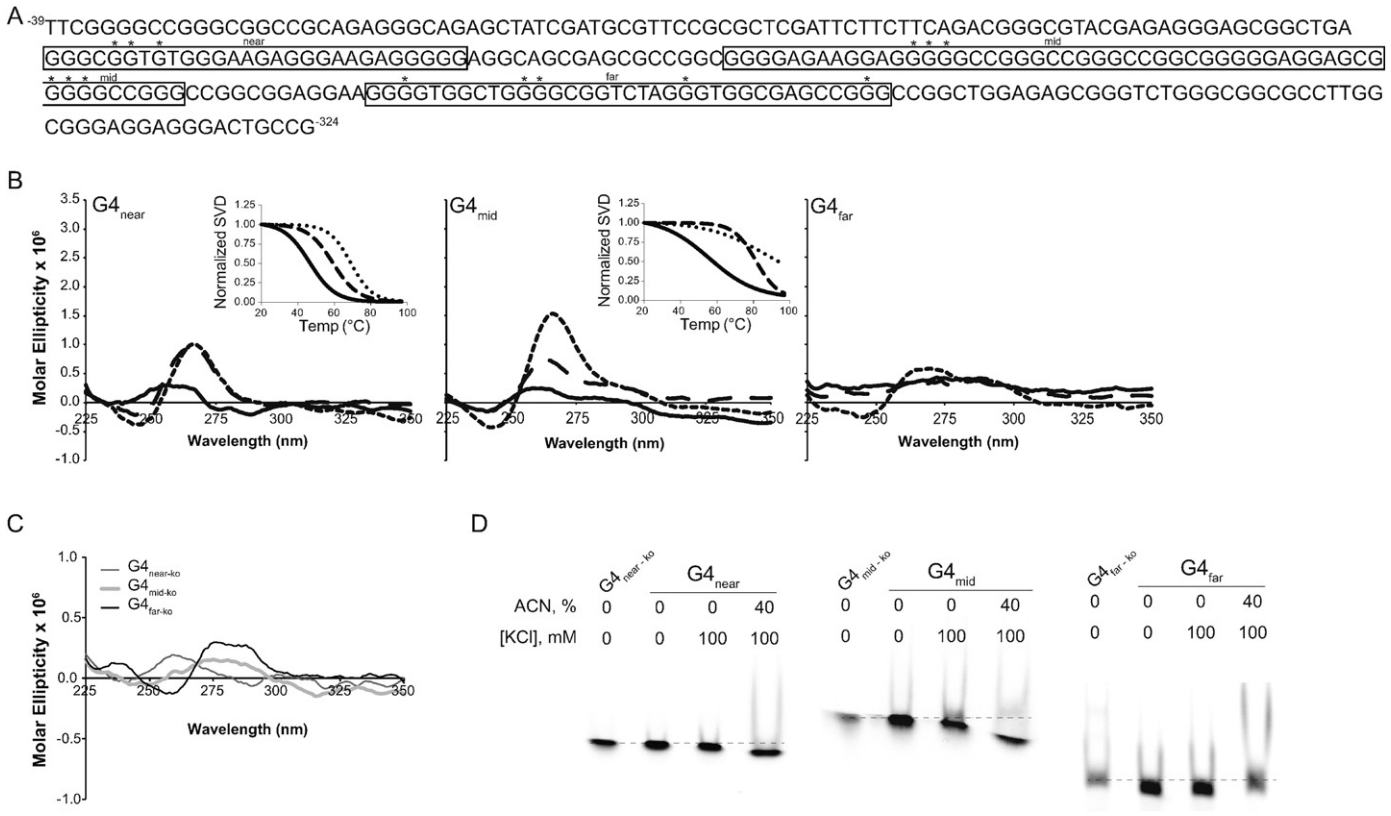

Fig. 1. G4 formations in the extended *kRAS* promoter region. (A) The *kRAS* promoter shown from −324 to −39 bp relative to the transcriptional start site, contains three distinct guanine-rich regions (boxed), termed near, mid, and far in the 5′–3′ direction. * denote G-to-T mutations within each region for knockout mutations shown in (C). (B) CD was used to determine G4 formation and stability within each of these G4-forming regions in the absence (solid line) or presence of 100 mM KCl alone (long dash line) or in the presence of 40% acetonitrile (ACN) (short dash line). Thermal stability from 20 to 100 °C is shown in the insets. (C) CD demonstrated a lack of inducible G4 formation in the presence of 100 mM KCl within each region with the selected G-to-T mutations in the knock-out (ko) sequences. (D) Electromobility shift assays were used to demonstrate the inter- versus intra-molecular G4 formations within each G4-forming region in the presence of 100 mM KCl with or without 40% ACN. A downward shifting of the DNA with the $G4_{near}$ and $G4_{mid}$ sequences, as compared to their linear ko sequences, indicates intramolecular structure formation, particularly evident in the presence of both cationic strength and dehydration. The $G4_{far}$ sequence, in the absence and presence of 100 mM KCl, demonstrates a downward shift from the linear ko sequence, but there is no difference between these two solvent conditions. In contrast, in the presence of KCl and ACN, there is a lack of a downward shift and the presence of retarded migration, as compared to control and KCl alone, indicating the potential for intramolecular G4 species.

G4 formation and overall stability of the near-, mid-, and far-regions were examined by CD, each in the absence and presence of intramolecular G4-stabilizing KCl alone or with 40% anhydrous acetonitrile (Fig. 1B). As noted in previous publications, $G4_{near}$ consists of a stable all-parallel structure as noted by the positive spectral maxima at 262 nm in the presence of KCl with or without ACN. In the presence of KCl, the thermal stability of this structure increased from 46 to 59 °C, and increased again to 69 °C with the addition of ACN. The mid-region forms a mixed parallel and antiparallel structure ($G4_{mid}$) as noted with the positive spectral maxima present at 263 and 290 nm, respectively. Thermal stability increases from 56 °C in solution alone, to 82 and over 95 °C in the presence of 100 mM KCl without and with 40% ACN, respectively. The far-region does not form a strong G4 structure, and spectral maxima suggesting that parallel and antiparallel orientations are only notable in the presence of both KCl and ACN; these structures were too weak to have thermal stability determined.

G-to-T knockout mutations were introduced into each G4-forming region (Table 1), and their higher order DNA formations were examined by CD in the presence of 100 mM KCl (Fig. 1C). As predicted the G-to-T mutations disrupted ($G4_{near\text{-}ko}$, mutation confirmed by DMS footprinting below) or abrogated ($G4_{mid\text{-}ko}$ and $G4_{far\text{-}ko}$) G4 formations. These sequences were used in EMSA analysis below to indicate migration of the linear species.

Electromobility shift assay (EMSA) was utilized to examine the inter-, versus intra-, molecular G4 formations (Fig. 1D). Sequences with G-to-T knockout mutations introduced and examined above were used as linear reference strands; dashed lines drawn horizontally indicate the migration pattern of linear DNA for each sequence. For both the near and the mid-regions, in the presence of 100 mM KCl alone a downward shift is evident, and the addition of 40% ACN makes the shift more marked. These faster migrations support the formation of smaller G4 structures under these conditions. The $G4_{far}$ sequence in the absence and presence of 100 mM KCl migrates lower than the linear knockout band, but there is no remarkable difference between those two. The addition of 40% ACN to this sequence retards migration of the DNA to be at or above the linear mark. Combined with CD data above, the $G4_{far}$ sequence is most likely forming a mixed parallel/antiparallel intermolecular structure under the combined conditions of cationic strength (KCl) and dehydration (ACN). The far region, by all data collected, is unlikely to form a significant intramolecular structure, and it was not examined any further.

3.2. Clarification of $G4_{near}$ isoforms from the complete 32-nucleotide region

In an effort to refine the predominant G4 isoform forming from the sequence at −129 bp from the TSS, biophysical characterization was performed on the 32 nucleotide sequence 5′-AGGGCGGTGTGGGAAG AGGGAAGAGGGGGAGG (Fig. 2A). This was undertaken in order to clarify the array of previously reported structures that vary in their guanine runs and inclusion of flanking regions [20–23,35]. In particular, DMS footprinting of the wild-type and two G-to-T mutant sequences demonstrated the major guanines used in the predominant isoform (Fig. 2B). In the presence, as compared to the absence, of KCl, the DMS cleavage pattern for the induced G-quadruplex in the WT sequence revealed a

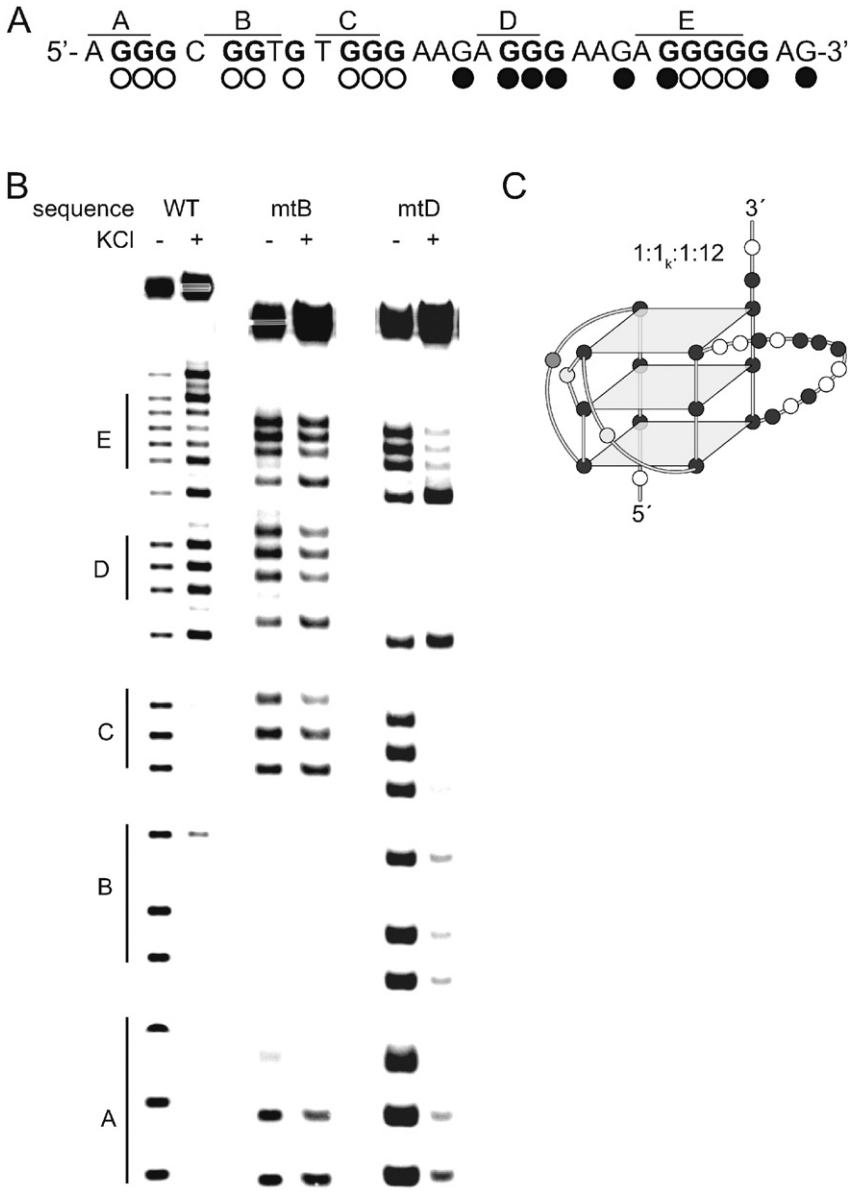

Fig. 2. Predominant G4 isoforms formed within the near kRAS promoter. (A) The $G4_{near}$ sequence contains four runs of continuous guanines – A, C–E – and one discontinuous run — B. The open circles indicate evidence of protection in the subsequent DMS footprinting, whereas the black circles indicate no protection or even hypercleavage from DMS labeling. (B) DMS footprinting of the near promoter region of kRAS in the presence (+) or absence (−) of 100 mM KCl was performed with the wild-type (WT) or select G-to-T mutations in run B (mtB) or D (mtD) sequences. In the absence of KCl, all guanines were labeled; upon the addition of 100 mM KCl, a protection pattern emerges in the WT sequence demonstrating a lack of DMS labeling of guanines in runs A–C and E. As this was an unusual pattern, runs B and D were individually mutated and those sequences were subject to DMS footprinting. G-to-T mutations of the discontinuous guanines in run B abrogated a clear protection pattern, whereas G-to-T mutations of the apparently non-incorporated run D were inconsequential to G4 formation. (C) Cumulatively, these data with the whole WT and select mt sequences were compiled to model a "kinked" thymine G4, including 5′–3′ loop sizes of 1, 1 kinked thymine, 1, and 12 bases. G = black circles, C = dark gray circles, T = light gray circles, A = white circles.

strong utilization of guanine runs A–C, and equilibrating utilization of the guanines in run E with a preference for the central three. Run D appears to be hyper-reactive to DMS, as compared to the absence of KCl (Fig. 2B, left). Due to the unique incorporation of a discontinuous guanine run (B), despite the presence of a possible fourth continuous guanine run (D), footprinting was also done on mtB and mtD sequences harboring G-to-T mutations within the runs indicated. When run B was mutated, the guanine protection pattern was disrupted and no higher order structure was noted; mutations of run D, however, maintained a pattern of guanine protection that was consistent with the WT sequence (Fig. 2B). These data, cumulatively with the CD findings from Fig. 1B–C, support modeling the predominant G4 formed from this 32-nucleotide region as an all parallel $1{:}1_k{:}1{:}12$ loop isomer, with the 1_k indicating the kinked thymine in run B between guanines (Fig. 2C). Collectively these data support that the kinked structure shown in the literature [23] is indeed the predominant isoform within the entire $G4_{near}$-forming-region.

3.3. Analysis of major G4's formed within the mid-region of the kRAS promoter

The 54-nucleotide mid-G4-forming region of the kRAS promoter contains seven unique runs of three or more continuous guanines, termed A–G in the 5′–3′ direction (Fig. 3A). DMS footprinting was performed on the entire wild-type $G4_{mid}$ sequence without and with 100 mM KCl; histograms of the banding patterns were obtained with ImageJ software. It is clear that a number of higher order structures

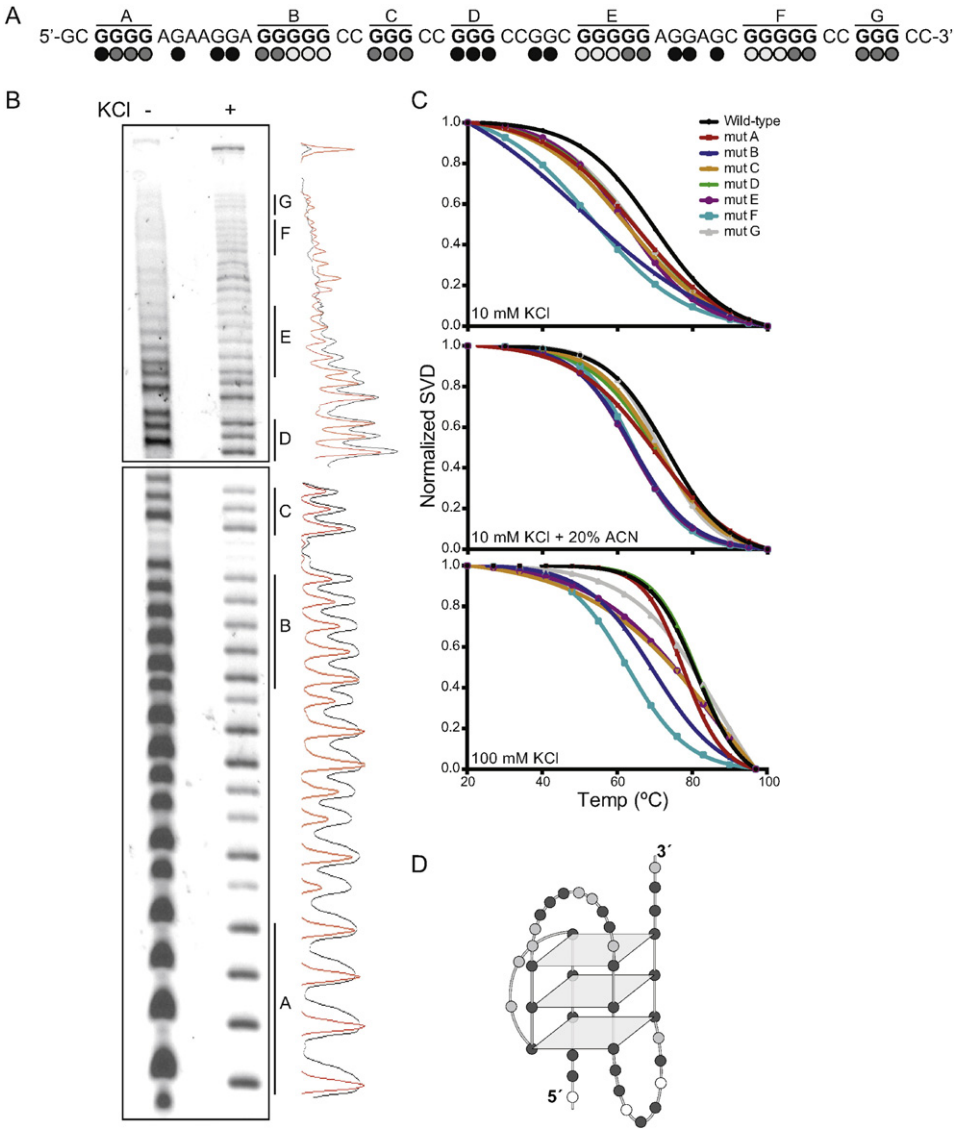

Fig. 3. Predominant G4 isoforms formed within the mid-region of the kRAS promoter. (A) The $G4_{mid}$ sequence contains seven runs of continuous guanines, A–G. The light gray circles indicate marked protection, the medium gray circles indicate partial protection, and the black circles indicate DMS-mediated piperidine cleavage. The open circles indicate evidence of protection in the subsequent DMS footprinting, whereas the black circles indicate no protection or even hypercleavage from DMS labeling. (B) DMS footprinting of the mid-promoter region of kRAS in the presence (+) or absence (−) of 100 mM KCl was performed with the wild-type (WT) sequence. Images obtained from the top and bottom portions of the sequencing gel (boxed individually) were aligned, ImageJ software was used to graph and align histograms of the guanine cleavage pattern (right, no KCl = black line; 100 mM KCl = red line). (C) Thermal stability of a series of G-to-T mutants interrupting runs A–G, individually, of the $G4_{mid}$ sequence was studied in the presence of 10 mM KCl alone (top), in the presence of 20% ACN (middle), or with 100 mM KCl (bottom). (D) Cumulatively, these data were used to predict a G4 isoform formation of a tri-stacked structure incorporating runs B, C, E and F with intervening loops of 2, 10, and 8 bases in the 5′–3′ direction. G = black circles, C = dark gray circles, T = light gray circles, A = white circles.

are forming in equilibrium, with at most only partial protection patterns clear in runs B, E and F (Fig. 3B).

To aid in the preliminary description of the $G4_{mid}$ structure, a series of single run knockout G-to-T mutations was made such that each run of continuous guanines was disrupted. These mutants were then examined by CD spectral and thermal analysis in conditions of varying cations and dehydration stabilities in order to probe the most relevant guanine runs involved in the predominant structure (Fig. 3C). In particular, the sequences were studied in 10 mM KCl, 10 mM KCl + 20% acetonitrile, and 100 mM KCl (Table 2). All structures demonstrate mixed loop directionality by CD with maxima in the parallel (260–264 nm) and antiparallel (~290 nm) ranges (data not shown). Consistently, in all conditions, mutations of runs B, E, and F destabilized the G4 structure, as evidenced by a decrease in the melt temperatures or a marked change in the slope of the melting profile, which indicates a change in the predominant isoforms (Fig. 3C). Melting profiles were examined in 100 mM KCl + 40% ACN conditions as well, but due to the extremely high thermal stability, T_Ms were indeterminate; the trends in mutant effects on overall G4 stability were comparable with the lower KCl and ACN conditions (data not shown). Taking the CD and DMS data together, a major isoform noted under the various conditions has been proposed utilizing

Table 2
Melting temperatures for $G4_{mid}$ sequences.

	Wild-type	Mut A	Mut B	Mut C	Mut D	Mut E	Mut F	Mut G
10 mM KCl	70	65	50	63	65	63	53	65
10 mM KCl + 20% ACN	73	70	64	71	71	64	64	71
100 mM KCl	81	78	70	89	82	84	63	87

runs B, C, E and F as a triple stacked tetrad with intervening loops of lengths 2, 10, and 8 in the 5′–3′ direction, respectively (Fig. 3D).

3.4. Biological function of various G4s within the entire kRAS promoter

Previous literature has described kRAS promoter silencing in the presence of TMPyP4 [20,33], which we used along with its positional isomer TMPyP2 to evaluate the biological function of the near- and mid-G4-forming regions of the kRAS promoter. The effect of each cationic porphyrin on the thermal stability of the $G4_{near}$ and $G4_{mid}$ structures was determined by FRET melt (Fig. 4A). Consistently, 1 μM TMPyP2 did not stabilize either structure, while 1 μM TMPyP4 did. In particular, the T_M of $G4_{near}$ was 34 °C alone and in the presence of TMPyP2, but increased to 65 °C in the presence of TMPyP4. Similarly, $G4_{mid}$'s T_M of 52 °C alone, or 46 °C in the presence of TMPyP2, was notably increased by TMPyP4 to 73 °C. While TMPyP4 does not show a preference to either G4 structure, it is a useful study tool to examine G4-mediated silencing of the kRAS promoter, with TMPyP2 as a negative control compound.

The effect of each compound on cellular viability and kRAS regulation was monitored in Panc-1 pancreatic cancer cells, which are often used in kRAS studies and particularly in previous G4 studies of the kRAS promoter [20,21,23,36]. Changes in Panc-1 cellular viability were monitored with the MTS assay at concentrations up to 500 μM incubated with the cells for 48 h. As both of these compounds have a marked absorbance in the same range as formazin (e.g. 490 nm), the assay was performed both subtracting for the colorimetric contribution of matched doses of TMPyP2 and TMPyP4 (termed pre-wash) and after removing all media from the 96 well plates and replacing it in all wells with fresh media before the addition of MTS + 5% PMS (termed post-wash); background corrections were still made for the lingering colorimetric effects of the compounds. Once the corrections were made for compound, it is evident from the post-wash conditions that at the concentrations utilized in all future experiments, namely 25 and 50 μM, there is no effect on Panc-1 cellular viability. Moreover, at concentrations up to 500 μM, TMPyP2 does not significantly impact Panc-1 cells, and TMPyP4 only decreases viability by approximately 25% (Fig. 4B). Panc-1 cells were incubated with 25 μM TMPyP2 or TMPyP4 for 48 h, and changes in kRAS mRNA expression were determined by qPCR. TMPyP4 significantly ($p < 0.05$) decreased kRAS expression to 45.0 ± 0.1% of control expression, whereas TMPyP2 had no significant effect (Fig. 4C). These findings support the role of G4-mediated silencing of kRAS expression.

In order to assess the contribution of $G4_{near}$ and $G4_{mid}$ to the silencing of kRAS transcription, a series of luciferase promoters was constructed (Fig. 5A). In particular, regions of the kRAS promoter were inserted into the promoterless pGL4.17 firefly luciferase plasmid (empty vector = EV). Following previously published methods [34] we assembled a plasmid (kRAS-500) containing the promoter region of kRAS from −500 to +0 in relation to the TSS, which had been shown to contain silencing G4s [33]. In addition a plasmid was assembled containing −324 to +50 in relation to the TSS (kRAS-324) to contain the near, mid, and far-G4-forming region and to include the immediate post-transcriptional region, which had previously been shown to be critical for full promoter activity [9–11]. In addition, G-to-T mutations were introduced in either the near- (324 mt Near) or mid- (324 mt Mid) G4-forming region. These mutations matched those from the knockout oligonucleotides in Fig. 1C. EV and an SV40-driven pGL4.13 firefly luciferase plasmid were used as control vectors for all experiments.

Basal expression from all plasmids was measured at 48 h, and firefly expression was normalized to pRL-driven renilla luciferase expression (Fig. 5B). SV40-promoter driven expression is almost 50-fold greater than activity from the promoterless EV (1.46 ± 0.08 versus 0.03 ± 0.01, respectively). The kRAS promoter plasmids fell in between these two control plasmids, and did not vary significantly from each other. In particular, kRAS-500 basal expression was 0.69 ± 0.11 and kRAS-324 was 0.94 ± 0.16. Each of these plasmids was also transfected into HEK-293 cells, which were then exposed to 25 μM TMPyP2 or TMPyP4

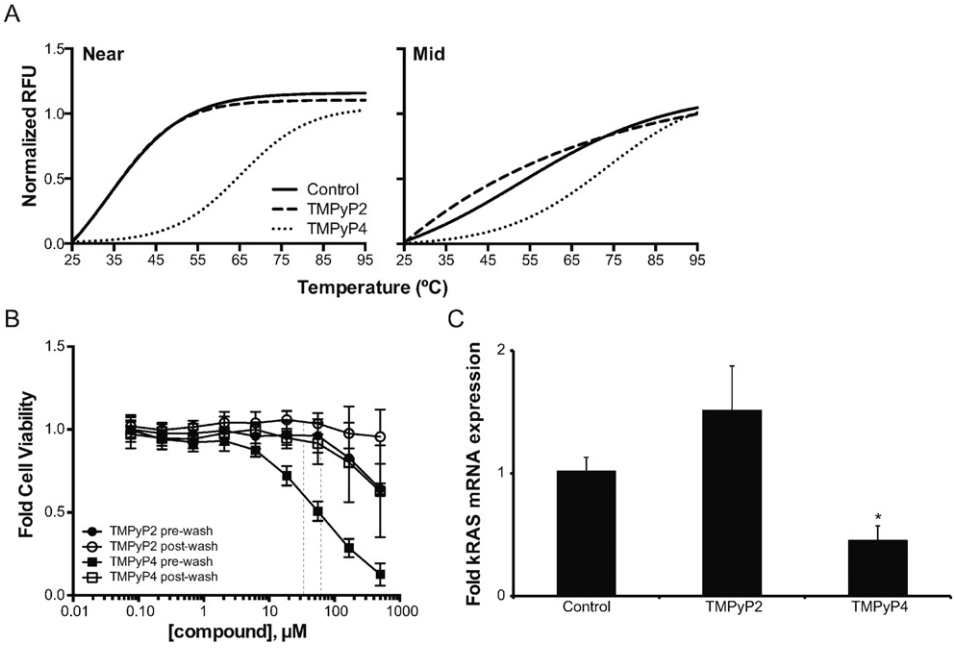

Fig. 4. Effect of G4 stabilization on pancreatic cancer cell viability and kRAS mRNA expression. (A) FRET Melt demonstrated a marked stabilization of both the $G4_{near}$ and the $G4_{mid}$ formations by the pan-G4-stabilizing TMPyP4 (1 μM), but not the inactive positional isomer TMPyP2 (1 μM). (B) The effect of each compound on pancreatic cancer cell, Panc-1, viability was measured at 48 h. MTS assays were done with plates where the subtracted background included compounds (pre-wash) and a series in which the media with and without compound was removed and was replaced with fresh media only, and subsequently included in the background normalization (post-wash). Due to the contribution of compound to the absorbance at 490, this washing even had a marked effect on the fold cell viability. Post-washing, neither TMPyP2 nor TMPyP4, at doses up to 500 μM, decreased cellular viability by 50%. Doses used in subsequent cellular assays are denoted by vertical dotted lines at 25 and 50 μM. (C) Panc-1 cells were incubated with 25 μM of either TMPyP2 or TMPyP4 for 48 h; subsequently kRAS mRNA, as normalized to GAPDH, was measured. TMPyP4, but not TMPyP2, significantly (*$p < 0.05$) decreased transcription and supported the presence of G4-mediated silencing of kRAS expression. Experiments were done in a minimum of triplicate; one-way ANOVA with Tukey post-hoc analysis was used to determine significance in (C).

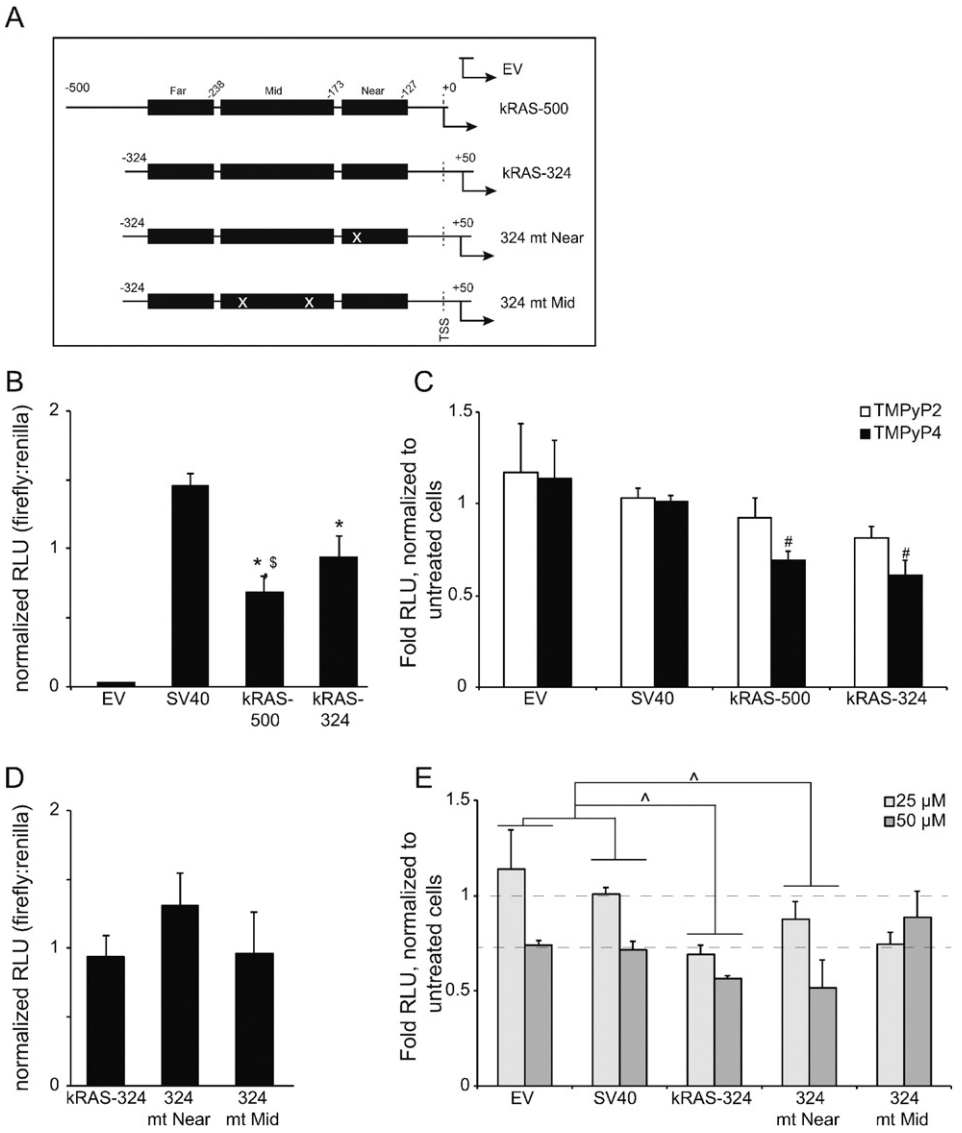

Fig. 5. Isolating silencing G4 formations within the *kRAS* promoter. (A) A series of luciferase plasmids was constructed from the promoterless empty vector (EV) pGL4.17 backbone to localize the silencing G4s within the kRAS promoter. These included kRAS-500 (−500 to +0, relative to the transcriptional start site (TSS)), and kRAS-324 (−324 to +50 relative to the TSS). Site-directed mutagenesis of kRAS-324 was used to introduce G-to-T mutations (approximate location indicated with white x) that abrogate $G4_{near}$ (324 mut Near) or $G4_{mid}$ (324 mt Mid) formation. (B) Basal expression of the non-mutated plasmids was examined in transiently transfected HEK-293 cells for 48 h and normalized to renilla expression in co-transfection assays. Promoterless (EV) and constitutively active (SV40) plasmids were included as comparison. There was no significant difference between the kRAS promoter plasmids. $^{*}p < 0.05$ as compared to EV, $^{\$}p < 0.05$ as compared to SV40 plasmid, as determined by one-way ANOVA. (C) The effects of HEK-293 treatment (48 h) with 25 μM TMPyP2 and TMPyP4 on promoter activity was examined in the EV, SV40 and wild-type kRAS promoter containing plasmids kRAS-500 and kRAS-324. TMPyP4 was equally significant ($^{\#}p < 0.05$ as compared to untreated control, per plasmid, as determined by one-way ANOVA) in lowering promoter activity in the two kRAS promoter plasmids, whereas it was inactive in the non-G4-containing EV and SV40 plasmids at that concentration. TMPyP2 was also inactive in all plasmids. (D) 48 h basal expression was examined from the 324 series of kRAS promoter plasmids, including wild-type kRAS-324, and select G4-knockout mutants 324 mt Near and 324 mt Mid. No change in basal expression was noted between any of these plasmids. (E) A TMPyP4 dose response (25 and 50 μM) was performed in the wild-type kRAS-324 plasmid and its two generated mutant plasmids 324 mt Near and 324 mt Mid. The dose response was performed in the non-G4-containing EV and SV40 plasmids. The colorimetric contribution of 50 μM TMPyP4 is evident in the EV and SV40 containing plasmids. In all plasmids where a dose–response was evident, the magnitude of that response was examined by a two-way ANOVA. Both kRAS-324 and 324 mt Near maintained significant ($\hat{}p < 0.05$ for dose response, as compared to EV and SV40 effects) G4-mediated silencing of promoter activity, whereas 324 mt Mid did not. These findings indicate that G4-mediated silencing is contained within the mid-guanine-rich region of the kRAS promoter. All experiments were performed in a minimum of triplicate.

for 48 h (Fig. 5C). There was no significant change in promoter activity for any plasmid when exposed to TMPyP2, nor was there any effect of TMPyP4 on the EV or SV40 plasmids. However, both kRAS-500 and kRAS-324 demonstrated significantly lower promoter activity with TMPyP4 treatment; the decreased promoter activity was the same for both plasmids. As all G4-silencing potential is housed within the 324 bp from the TSS, and the kRAS-324 plasmid contains the previously reported critical +50 bp region downstream of the TSS [9–11], further studies were done using this plasmid.

As described above, site-directed mutagenesis was used to introduce G-to-T mutations to the near- and mid-G4 forming regions such that higher order DNA structures could not form (as confirmed in Fig. 1C), while minimizing disruptions to potential transcription factor binding sites. Basal expression was measured from each of the 324 plasmids after 48 h of transfection, and there were no significant differences between any plasmids (Fig. 5D). In particular, as compared to the kRAS-324's expression of 0.94 ± 0.16, the expression for 324 mt Near and 324 mt Mid was 1.31 ± 0.23 and 0.96 ± 0.30, respectively. Upon the addition of TMPyP2, as for all plasmids described above, no significant changes occurred with any plasmid with fold RLU of 0.99 ± 0.10 and 1.01 ± 0.08 for 324 mt Near and 324 mt Mid, respectively.

Upon exposure of the plasmids to 25 and 50 μM TMPyP4, a number of significant effects were noted (Fig. 5E). Specifically, higher concentrations of TMPyP4 led to an apparent decrease in luciferase activity or in luciferin light detection as evidenced by the significant change in fold RLU from both the EV and SV40 plasmids exposed to 50 μM compound to 0.75 ± 0.05 and 0.72 ± 0.04, respectively. The dose–response noted in EV and SV40 plasmids was comparable, and was considered to account for background effects of TMPyP4. This non-specific effect is most likely due to dampening of the luciferin glow by the cationic compound, in agreement with a previous study showing the same decreased RLU but no transcriptional downregulation from the EV plasmid treated with 100 μM TMPyP4, as measured by PCR [37]. Any significant changes in the extent of the dose response were compared to these background effects using a two-way ANOVA. Both the kRAS-324 and the 324 mt Near, but not the 324 mt Mid, plasmids had significantly ($p < 0.05$) different dose–responses than the control plasmids. At the highest dose, fold RLU was decreased to 0.55 ± 0.09 and 0.51 ± 0.15 for the kRAS-324 and 324 mt Near plasmids, respectively, and was 0.89 ± 0.14 for the 324 mt Mid plasmid. When the fold RLU is normalized to the EV and SV40 non-specific effects, a 26 and 30% decrease in RLU was observed for the kRAS-324 and 324 mt Near plasmids, respectively, while the 324 mt Mid plasmid displayed a 21% increase in RLU. For comparison, at the same concentration of TMPyP4, the MYC promoter-containing Del4 plasmid [38,39] demonstrated a fold RLU of 0.56 ± 0.13, for a 24% decrease as compared to the EV and SV40 plasmid non-specific effects (data not shown). From these data, we conclude that within the entire kRAS core promoter, the most critical higher order DNA structure related to transcriptional silencing is the $G4_{mid}$ structure, as its abrogation disrupts TMPyP4-mediated promoter downregulation, and it is a new molecular structure for the development of targeted therapeutics.

4. Discussion

The current work has characterized an extensive guanine-rich region of the kRAS core promoter, extending out 500 base-pairs past the transcriptional start site. Within this region, of the three distinct putative G-quadruplex (G4)-forming areas, the most proximal and the medial regions, termed near and mid, respectively, formed inducible structures under a variety of buffer conditions, whereas the most distal region, termed far, did not. Much more critically, a series of experiments probing the potential biological role of G4 formation within cells highlighted the silencing function to be maintained predominantly in the mid-region, versus in the previously described near structure. Initial probing indicates that a great number of competing isoforms exist in equilibrium under ex vivo conditions, and suggest that a major $G4_{mid}$ structure is a tri-stacked mixed parallel and antiparallel isoform utilizing the second, third, fifth, and sixth runs of continuous guanines with loop lengths of up to 10 nucleotide. Extensive characterization work is ongoing to narrow the equilibrating isoforms under a variety of physiological conditions, including molecular crowding, dehydration, and torsional stress.

The core promoter region of kRAS is highly G/C-rich (~75%) and contains two nuclease hypersensitivity elements housing the described G4-forming regions [9–11]. Notably, the region +/− 50 bp surrounding the TSS is critical for directing and initiating transcription. The further upstream elements, including the DNase-sensitive G4-forming regions, are important for optimal kRAS expression and are capable of dampening promoter activity, but are not the main initiator regions for transcription [11]. Mutation of biologically active G4 structures within critical core promoters generally leads to a change in basal promoter activity [40,41]. No such observation was made in the current study with mutation of either the near or the mid-G4 structure in the current study, which is in agreement with the previous description of the upstream promoter region.

The physical binding of transcription factors to the kRAS promoter region has not been mapped, making it difficult to assess the potential impact of mutating potential transcription factor binding sites. The core promoter +/− 50 surrounding the TSS contains one consensus Sp1 binding site, five E2F-1 sites (four of which are in the critical region from 0 to +50 bp), and consensus sites for a number of other factors, including WT1, GR-alpha, p53, STAT4, and NF-AT1/2. The near- and mid-G4-forming regions each contain a number of putative transcriptional regulator binding sites as well, including two for MAZ (one at the end of the near region and one in the midst of the mid-region), three for Sp1 (one in the near region and two within the mid-region), and several for p53, E2F-1, STAT4, WT1, NF-kB, and more. The G-to-T mutations introduced to the mid-G4 region disrupted predicted transcription factor binding sites for p53, ETF, E2F1, and WT1. Mutation of the near-G4 region interrupted putative binding sites for Sp1 (one of six within the kRAS-324 plasmid), p53 and E2F. It is possible that the disruption of transcription factor binding sites within these regions could lead us to underestimate the silencing potential of each G4-forming region, as the expected increase in promoter activity due to G4 mutation would be dampened by a loss of transcription factor binding. When the disruption of G4 formation is considered, however, along with the observed effects of TMPyP4 with the WT and each mutant plasmid, the likelihood of a significant silencing effect of the mid-G4 is high and that of the near-G4 is low.

The near region has been extensively explored by Xodo's group [20–23,35], with variations in nucleotide inclusion, leading to evolving molecular models. These models varied from a di- to a tri-tetrad stack, altering loop lengths and directionality. Initially, 2 isoforms were proposed — both parallel three-tetrad G4s with a kinked cytosine located between the first and second guanine runs [21]. In subsequent publications, the models were re-configured and inclusion of a thymine in run two was suggested by [20]. The first model containing the possibility of a kinked thymine in the second guanine run was noted in 2009 with the inclusion of T/G (at the published positions 8/9) [23], and a more concrete description of the hypothesized isoform was offered in 2011 as a supplementary model [22]. Given the varying models and sequences, the present work included clarification of the particular guanines involved in structure formation from the near-G4-forming region in a more inclusive sequence, and confirmed the "kinked" structure as the predominant isoform.

Surprisingly, further examination into the biological function of this near sequence, in the context of the human core promoter, demonstrated a lack of silencing potential. This is in contrast to the conclusions of a 2006 study in which transfection of the human kRAS $G4_{near}$ promoter sequence along with a CAT plasmid driven by the mouse kRAS promoter sequence indicated silencing potential [21]. The previous experiment examined the effect of transfecting wild-type and knockout mutant $G4_{near}$ on the promoter activity from the mouse sequence (with 60–70% homology to the human sequence [11]), whereas the current study directly examines the human sequence with wild-type and specific $G4_{near}$, in addition to $G4_{mid}$, knockout mutations within the entire core kRAS promoter. While initial reports indicated a role of $G4_{near}$ in silencing kRAS expression, as this was never directly examined within the context of the human sequence, the results presented herein are more accurate assessments of the biological function. These reports are not in disagreement, but are rather comparing different outcomes.

It is important to note that the data supporting G4-mediated-silencing of the kRAS promoter to be housed in the mid-G4-forming region does not negate other important findings regarding G4 formation within the kRAS promoter. In particular, work with TMPyP4 suggested a decrease in kRAS expression within the first 500 bp from the TSS [33], which we confirmed and clarified further to exist within the first 324 bp. Additionally, there are a number of studies working with protein regulation of the kRAS promoter [20,23,42], and the use of structurally unrelated G4-decoys that have in vitro and in vivo efficacy [35,36] highlighting the function of G4 formation. Rather, we hypothesize that

the G4-mediated events noted in these other works in cells are mediated through the silencing G4 identified in the current works in the mid-G4-forming region. There are a number of similar sequences and consensus binding sites for the same transcription factors [9–11], further in support of this hypothesis.

kRAS is frequently mutated in multiple cancer types, especially in pancreatic cancer, making it a good anti-cancer target. The very low survival rate of pancreatic cancer patients clearly indicates that new and more efficacious treatments are needed and targeted kRAS dowregulation holds a great deal of promise. Efforts have been made to develop clinical agents focused on kRAS such as targeting its membrane localization with farnesyltransferase inhibitors (FTIs), or its downstream effectors, such as Raf kinase, MEK, and mTOR [43,44]. Unfortunately, none of these strategies have shown clinical efficacy. It is notable that specific inhibition of kRAS expression using antisense or siRNA oligonucleotides has shown promising preclinical activity, but their application in the clinic is hampered by difficulties in drug delivery [6,7]. The characterization of a unique DNA structure, as described herein, allows for a new area of therapeutic research focused on small-molecule mediated downregulation of kRAS expression. The identification of small molecules that can interfere with *kRAS* transcription by stabilizing G4s, will combine the best of all approaches — the specific downregulation of kRAS expression with the benefit of ease of delivery, as compared to antisense oligos. Thus, such small molecules will have great potential in ultimately achieving clinical activity in patients whose tumors have harbored this dysregulated oncogene.

Putative G4 forming regions of DNA are preferentially clustered ~1 Kb upstream of the transcriptional start site [45]. Interestingly, these sequences are found more frequently in oncogenic promoters [12], including some representatives of the hallmarks of cancer [46]. The varying loop lengths and tetrad compositions of G4s allow for specific targeting, similar to targeting a protein with a unique tertiary structure. The targeting of G4 secondary structures within oncogenic promoter regions has led to the development of two agents which advanced into clinical trials: the first-in-class small molecule Quarfloxin by Cylene Pharmaceuticals, which was halted at phase II clinical development due to difficulties with delivery and excessive albumin binding, and antisoma's G-rich phosphodiester oligonucleotide AS1411, a DNA aptamer with rare, but durable activity in renal cell carcinoma, with minimal associated toxicities [47].

We have identified and characterized a previously unexamined region of the kRAS promoter that is capable of forming a stable G4, of which stabilization by the cationic porphyrin TMPyP4 led to a significant decrease in promoter activity in an isolated plasmid system and in whole cells. TMPyP4 is a promiscuous G4-binding compound, although not of particular potency; its effect on kRAS promoter activity was consistent with the effect on the MYC promoter-containing Del4 plasmid, as noted in the Results section. The MYC structure is the most well described promoter G4, with known silencer function [46,48]. Thus, the similarity of observed changes in promoter activity from these two plasmids supports the promise of targeting the kRAS mid-G4 for clinical gain. The work with G4 decoys modulating the kRAS promoter and affecting tumor growth in vivo, albeit prescribed to a less significant region of the promoter in the original publications, further highlights the potential G4-mediated regulation of kRAS transcription [35,36]. This guanine-rich region of the kRAS promoter represents a highly valuable new molecular target for the development of small molecule therapeutics aimed at a number of cancers harboring mutant kRAS, most notably pancreatic cancer.

Transparency document

The Transparency document associated with this article can be found in the online version.

Acknowledgment

U.S. Department of Defense PRCRP grant (to Brooks) CA130229, startup funds from the University of Mississippi (to Brooks).

References

[1] A.A. Adjei, Blocking oncogenic Ras signaling for cancer therapy, J. Natl. Cancer Inst. 93 (2001) 1062–1074.
[2] B.B. Friday, A.A. Adjei, K-ras as a target for cancer therapy, Biochim. Biophys. Acta 1756 (2005) 127–144.
[3] A. Young, J. Lyons, A.L. Miller, V.T. Phan, I.R. Alarcon, F. McCormick, Ras signaling and therapies, Adv. Cancer Res. 102 (2009) 1–17.
[4] Y. Pylayeva-Gupta, E. Grabocka, D. Bar-Sagi, RAS oncogenes: weaving a tumorigenic web, Nat. Rev. 11 (2011) 761–774.
[5] S.R. Hingorani, E.F. Petricoin, A. Maitra, V. Rajapakse, C. King, M.A. Jacobetz, S. Ross, T.P. Conrads, T.D. Veenstra, B.A. Hitt, Y. Kawaguchi, D. Johann, L.A. Liotta, H.C. Crawford, M.E. Putt, T. Jacks, C.V. Wright, R.H. Hruban, A.M. Lowy, D.A. Tuveson, Preinvasive and invasive ductal pancreatic cancer and its early detection in the mouse, Cancer Cell 4 (2003) 437–450.
[6] A.M. Duursma, R. Agami, Ras interference as cancer therapy, Semin. Cancer Biol. 13 (2003) 267–273.
[7] E. Wickstrom, Oligonucleotide treatment of ras-induced tumors in nude mice, Mol. Biotechnol. 18 (2001) 35–55.
[8] K. Podsypanina, K. Politi, L.J. Beverly, H.E. Varmus, Oncogene cooperation in tumor maintenance and tumor recurrence in mouse mammary tumors induced by Myc and mutant Kras, Proc. Natl. Acad. Sci. U. S. A. 105 (2008) 5242–5247.
[9] J. Jordano, M. Perucho, Chromatin structure of the promoter region of the human c-K-ras gene, Nucleic Acids Res. 14 (1986) 7361–7378.
[10] J. Jordano, M. Perucho, Initial characterization of a potential transcriptional enhancer for the human c-K-ras gene, Oncogene 2 (1988) 359–366.
[11] F. Yamamoto, M. Perucho, Characterization of the human c-K-ras gene promoter, Oncogene Res. 3 (1988) 125–130.
[12] A. Verma, K. Halder, R. Halder, V.K. Yadav, P. Rawal, R.K. Thakur, F. Mohd, A. Sharma, S. Chowdhury, Genome-wide computational and expression analyses reveal G-quadruplex DNA motifs as conserved cis-regulatory elements in human and related species, J. Med. Chem. 51 (2008) 5641–5649.
[13] J. Eddy, N. Maizels, Gene function correlates with potential for G4 DNA formation in the human genome, Nucleic Acids Res. 34 (2006) 3887–3896.
[14] G. Biffi, D. Tannahill, J. McCafferty, S. Balasubramanian, Quantitative visualization of DNA G-quadruplex structures in human cells, Nat. Chem. 5 (2013) 182–186.
[15] E.Y. Lam, D. Beraldi, D. Tannahill, S. Balasubramanian, G-quadruplex structures are stable and detectable in human genomic DNA, Nat. Commun. 4 (2013) 1796.
[16] S. Muller, S. Kumari, R. Rodriguez, S. Balasubramanian, Small-molecule-mediated G-quadruplex isolation from human cells, Nat. Chem. 2 (2010) 1095–1098.
[17] V.S. Chambers, G. Marsico, J.M. Boutell, M. Di Antonio, G.P. Smith, S. Balasubramanian, High-throughput sequencing of DNA G-quadruplex structures in the human genome, Nat. Biotechnol. 33 (2015) 877–881.
[18] C.K. Kwok, S. Balasubramanian, Targeted detection of G-quadruplexes in cellular RNAs, Angew. Chem. 54 (2015) 6751–6754.
[19] A. Shivalingam, M.A. Izquierdo, A.L. Marois, A. Vysniauskas, K. Suhling, M.K. Kuimova, R. Vilar, The interactions between a small molecule and G-quadruplexes are visualized by fluorescence lifetime imaging microscopy, Nat. Commun. 6 (2015) 8178.
[20] S. Cogoi, M. Paramasivam, B. Spolaore, L.E. Xodo, Structural polymorphism within a regulatory element of the human KRAS promoter: formation of G4-DNA recognized by nuclear proteins, Nucleic Acids Res. 36 (2008) 3765–3780.
[21] S. Cogoi, L.E. Xodo, G-quadruplex formation within the promoter of the KRAS proto-oncogene and its effect on transcription, Nucleic Acids Res. 34 (2006) 2536–2549.
[22] M. Paramasivam, S. Cogoi, L.E. Xodo, Primer extension reactions as a tool to uncover folding motifs within complex G-rich sequences: analysis of the human KRAS NHE, Chem. Commun. (Camb.) 47 (2011) 4965–4967.
[23] M. Paramasivam, A. Membrino, S. Cogoi, H. Fukuda, H. Nakagama, L.E. Xodo, Protein hnRNP A1 and its derivative Up1 unfold quadruplex DNA in the human KRAS promoter: implications for transcription, Nucleic Acids Res. 37 (2009) 2841–2853.
[24] R. Hänsel, F. Löhr, S. Foldynová-Trantirková, E. Bamberg, L. Trantirek, V. Dötsch, The parallel G-quadruplex structure of vertebrate telomeric repeat sequences is not the preferred folding topology under physiological conditions, Nucleic Acids Res. 39 (2011) 5768–5775.
[25] M.C. Miller, R. Buscaglia, J.B. Chaires, A.N. Lane, J.O. Trent, Hydration is a major determinant of the G-quadruplex stability and conformation of the human telomere 3′ sequence of d(AG(3)(TTAG(3))(3)), J. Am. Chem. Soc. (2010).
[26] L. Petraccone, Higher-order quadruplex structures, Top. Curr. Chem. 330 (2013) 23–46.
[27] X. Qu, J.B. Chaires, Contrasting hydration changes for ethidium and daunomycin binding to DNA, J. Amer. Chem. Soc. 121 (1999) 2649–2650.
[28] X. Qu, J.B. Chaires, Hydration changes for DNA intercalation reactions, J. Amer. Chem. Soc. 123 (2000) 1–7.
[29] J.W.R. Schwabe, The role of water in protein–DNA interactions, Curr. Opin. Struct. Biol. 7 (1997) 126–134.
[30] R.J. DeSa, I.B. Matheson, A practical approach to interpretation of singular value decomposition results, Methods Enzymol. 384 (2004) 1–8.

[31] A. De Cian, L. Guittat, M. Kaiser, B. Sacca, S. Amrane, A. Bourdoncle, P. Alberti, M.P. Teulade-Fichou, L. Lacroix, J.L. Mergny, Fluorescence-based melting assays for studying quadruplex ligands, Methods (San Diego, CA, U. S.) 42 (2007) 183–195.
[32] B.T. Mossman, In vitro approaches for determining mechanisms of toxicity and carcinogenicity by asbestos in the gastrointestinal and respiratory tracts, Environ. Health Perspect. 53 (1983) 155–161.
[33] J. Lavrado, H. Brito, P.M. Borralho, S.A. Ohnmacht, N.S. Kim, C. Leitao, S. Pisco, M. Gunaratnam, C.M. Rodrigues, R. Moreira, S. Neidle, A. Paulo, KRAS oncogene repression in colon cancer cell lines by G-quadruplex binding indolo[3,2-c]quinolines, Sci. Rep. 5 (2015) 9696.
[34] I.S. Song, N.S. Oh, H.T. Kim, G.H. Ha, S.Y. Jeong, J.M. Kim, D.I. Kim, H.S. Yoo, C.H. Kim, N.S. Kim, Human ZNF312b promotes the progression of gastric cancer by transcriptional activation of the K-ras gene, Cancer Res. 69 (2009) 3131–3139.
[35] S. Cogoi, M. Paramasivam, V. Filichev, I. Geci, E.B. Pedersen, L.E. Xodo, Identification of a new G-quadruplex motif in the KRAS promoter and design of pyrene-modified G4-decoys with antiproliferative activity in pancreatic cancer cells, J. Med. Chem. 52 (2009) 564–568.
[36] S. Cogoi, S. Zorzet, V. Rapozzi, I. Geci, E.B. Pedersen, L.E. Xodo, MAZ-binding G4-decoy with locked nucleic acid and twisted intercalating nucleic acid modifications suppresses KRAS in pancreatic cancer cells and delays tumor growth in mice, Nucleic Acids Res. 41 (2013) 4049–4064.
[37] R.V. Brown, V.C. Gaerig, T. Simmons, T.A. Brooks, Helping Eve overcome ADAM: G-quadruplexes in the ADAM-15 promoter as new molecular targets for breast cancer therapeutics, Molecules (Basel, Switz.) 18 (2013) 15019–15034.
[38] T.C. He, A.B. Sparks, C. Rago, H. Hermeking, L. Zawel, L.T. da Costa, P.J. Morin, B. Vogelstein, K.W. Kinzler, Identification of c-MYC as a target of the APC pathway, Science 281 (1998) 1509–1512.
[39] T. Lemarteleur, D. Gomez, R. Paterski, E. Mandine, P. Mailliet, J.F. Riou, Stabilization of the c-myc gene promoter quadruplex by specific ligands' inhibitors of telomerase, Biochem. Biophys. Res. Commun. 323 (2004) 802–808.
[40] J. Seenisamy, E.M. Rezler, T.J. Powell, D. Tye, V. Gokhale, C.S. Joshi, A. Siddiqui-Jain, L.H. Hurley, The dynamic character of the G-quadruplex element in the c-MYC promoter and modification by TMPyP4, J. Am. Chem. Soc. 126 (2004) 8702–8709.
[41] X.-D. Wang, T.-M. Ou, Y.-J. Lu, Z. Li, Z. Xu, C. Xi, J.-H. Tan, S.-L. Huang, L.-K. An, D. Li, L.-Q. Gu, Z.-S. Huang, Turning off transcription of the *bcl-2* gene by stabilizing the *bcl-2* promoter quadruplex with quindoline derivatives, J. Med. Chem. 53 (2010) 4390–4398.
[42] S. Cogoi, M. Paramasivam, A. Membrino, K.K. Yokoyama, L.E. Xodo, The KRAS promoter responds to Myc-associated zinc finger and poly(ADP-ribose) polymerase 1 proteins, which recognize a critical quadruplex-forming GA-element, J. Biol. Chem. 285 (2010) 22003–22016.
[43] J. Bendell, R.M. Goldberg, Targeted agents in the treatment of pancreatic cancer: history and lessons learned, Curr. Opin. Oncol. 19 (2007) 390–395.
[44] J.S. Macdonald, S. McCoy, R.P. Whitehead, S. Iqbal, J.L. Wade 3rd, J.K. Giguere, J.L. Abbruzzese, A phase II study of farnesyl transferase inhibitor R115777 in pancreatic cancer: a southwest oncology group (SWOG 9924) study, Investig. New Drugs 23 (2005) 485–487.
[45] J.L. Huppert, A. Bugaut, S. Kumari, S. Balasubramanian, G-quadruplexes: the beginning and end of UTRs, Nucleic Acids Res. 36 (2008) 6260–6268.
[46] T.A. Brooks, L.H. Hurley, The role of supercoiling in transcriptional control of MYC and its importance in molecular therapeutics, Nat. Rev. 9 (2009) 849–861.
[47] J.E. Rosenberg, R.M. Bambury, E.M. Van Allen, H.A. Drabkin, P.N. Lara Jr., A.L. Harzstark, N. Wagle, R.A. Figlin, G.W. Smith, L.A. Garraway, T. Choueiri, F. Erlandsson, D.A. Laber, A phase II trial of AS1411 (a novel nucleolin-targeted DNA aptamer) in metastatic renal cell carcinoma, Investig. New Drugs 32 (2014) 178–187.
[48] T.A. Brooks, L.H. Hurley, Targeting MYC expression through G-quadruplexes, Genes Cancer 1 (2010) 641–649.